

CONFIDENTIAL

CLASSIFIED

Copy
RM H56117

c.1

NACA RM H56117



RESEARCH MEMORANDUM

LONGITUDINAL STABILITY CHARACTERISTICS OF THE CONVAIR

YF-102 AIRPLANE DETERMINED FROM FLIGHT TESTS

By William H. Andrews, Thomas R. Sisk,
and Robert W. Darville

High-Speed Flight Station
Edwards, Calif.

LIBRARY COPY

DEC 18 1956

LANGLEY AERONAUTICAL LABORATOR
LIBRARY NACA
LANGLEY FIELD, VIRGINIA

CLASSIFIED DOCUMENT

This material contains information affecting the National Defense of the United States within the meaning of the espionage laws, Title 18, U.S.C., Secs. 793 and 794, the transmission or revelation of which in any manner to an unauthorized person is prohibited by law.

NATIONAL ADVISORY COMMITTEE FOR AERONAUTICS

WASHINGTON

December 13, 1956

UNCLASSIFIED

CLASSIFICATION CHANGED

UNCLASSIFIED

To
By authority of T.P.A. # 27 Date 7-28-66 JHA

CONFIDENTIAL

NATIONAL ADVISORY COMMITTEE FOR AERONAUTICS

RESEARCH MEMORANDUM

LONGITUDINAL STABILITY CHARACTERISTICS OF THE CONVAIR

YF-102 AIRPLANE DETERMINED FROM FLIGHT TESTS

By William H. Andrews, Thomas R. Sisk,
and Robert W. Darville

SUMMARY

An analysis was made of the longitudinal stability characteristics of the cambered-wing version of the Convair YF-102 airplane from flight data obtained up to a Mach number of 1.18 at altitudes of 25,000, 40,000, and 50,000 feet. In addition, trim data are analysed for the symmetrical-wing configuration at the two lower altitudes.

The longitudinal control for trim appears conventional, with the unstable region occurring generally in the Mach number range from 0.87 to 0.95. The cambered-wing modification reduced the elevator required for 1 g trim below that required with the original-wing configuration by approximately 0.6° to 1.9° at 25,000 feet.

The longitudinal damping characteristics met the Military Specification to damp to one-half amplitude in 1 cycle, but did not indicate that damping to one-tenth amplitude in 1 cycle could be attained. The pilots commented that the damping was insufficient.

Generally there was a gradual decrease in stability with increasing lift. However, no severe pitch-up tendencies were exhibited, except when accelerating or decelerating through the trim-change region. The stability more than doubles between Mach numbers of 0.60 and 1.16; however, the control effectiveness shows an increase up to a Mach number of 0.89 with a rapid decrease of approximately 50 percent occurring between Mach numbers of 0.90 and 1.0.

An abrupt decrease in the stick-free stability exhibited between 1.5g and 2.0g is felt to result from the location of the total head and static-sensing probes for the Mach compensating instrument of the artificial-feel system.

~~CONFIDENTIAL~~

INTRODUCTION

To evaluate the longitudinal stability and control characteristics and thus extend the present information on delta-wing airplanes, the National Advisory Committee for Aeronautics is conducting an extensive flight investigation with the Convair YF-102 airplane at the High-Speed Flight Station at Edwards, Calif.

The first portion of the flight program was performed with the original symmetrical-wing configuration. However, to improve the drag characteristics of the airplane, as reported in reference 1, the major and more recent part of the flight program was performed with the wing leading edge cambered and the wing trailing edge outboard of the elevons reflexed 10° up.

The tests were performed during steady and maneuvering flight over the entire speed range capabilities of the airplane up to a Mach number of 1.18 at altitudes of 25,000, 40,000, and 50,000 feet.

SYMBOLS

a_n	normal acceleration at center of gravity, g units
b	wing span, ft
$C_{1/2}$	cycles to damp to one-half amplitude
$C_{1/10}$	cycles to damp to one-tenth amplitude
C_m	pitching-moment coefficient, $\frac{\text{Pitching moment}}{\frac{1}{2}\rho V^2 S \bar{c}}$
C_{m_α}	static stability parameter, $\frac{dC_m}{d\alpha}$, per deg
$C_{m_{\delta_e}}$	elevator effectiveness parameter, $\frac{dC_m}{d\delta_e}$, per deg
C_{N_A}	airplane normal-force coefficient, $\frac{W a_n}{\frac{1}{2}\rho V^2 S}$

~~CONFIDENTIAL~~

$C_{N_{\alpha}}$	rate of change of airplane normal-force coefficient with angle of attack, per deg
c	wing chord, ft
\bar{c}	mean aerodynamic chord, ft
F_a	aileron stick force, lb
F_e	elevator stick force, lb
F_r	rudder pedal force, lb
g	acceleration due to gravity, ft/sec ²
h_p	pressure altitude, ft
I_x	moment of inertia about the longitudinal body axis, slug-ft ²
I_y	moment of inertia about the lateral body axis, slug-ft ²
I_z	moment of inertia about the normal body axis, slug-ft ²
I_{xz}	product of inertia, slug-ft ²
M	Mach number
P	period of longitudinal oscillation, sec
P_1	total-head pressure, lb/sq ft
P_2	static pressure, lb/sq ft
P_3	pneumatic pressure supplied to elevator feel force cylinder, lb/sq ft
p	rolling angular velocity, radians/sec
q	pitching angular velocity, radians/sec
\dot{q}	pitching angular acceleration, radians/sec ²
r	yawing angular velocity, radians/sec

S	wing area, sq ft
$T_{1/2}$	time to damp to one-half amplitude of longitudinal oscillation, sec
t	time, sec
V	true velocity, ft/sec
V_i	indicated velocity, knots
W	airplane weight, lb
α	angle of attack, deg
β	angle of sideslip, deg
δ_a	aileron control angle, $\delta_{e_L} - \delta_{e_R}$, right roll positive, deg
δ_e	elevator control angle, $\frac{\delta_{e_L} + \delta_{e_R}}{2}$, positive when trailing edge down, deg
δ_r	rudder control angle, positive when trailing edge left, deg
δ_{s_a}	transverse stick position, in.
δ_{s_e}	longitudinal stick position, in.
δ_p	rudder pedal position, in.
ρ	mass density of air, slug/cu ft
$\frac{dC_m}{dC_{N_A}}$	static margin
$\frac{dF_e}{da_n}$	rate of change of elevator stick force with normal acceleration, lb/g
$\frac{d\delta_e}{da_n}$	rate of change of elevator deflection with normal acceleration, deg/g

$\frac{d\delta_e}{dC_{N_A}}$ rate of change of elevator deflection with normal-force coefficient, deg

Subscripts:

L left
R right

AIRPLANE

The Convair YF-102 airplane, illustrated by the three-view drawing and photographs of figures 1 and 2, respectively, was designed as a high-performance, all-weather interceptor. It is a semitailless, delta-wing airplane having a 60° leading-edge sweepback of the wing and vertical tail. During the flight investigation, two wing configurations were tested. The original wing designed for the airplane employed a symmetrical airfoil with a 4-percent thickness ratio and outboard wing fences on the upper surface of the wing (fig. 1(b)). However, in the early stages of the flight program, the wing was modified by incorporating a 6.3-percent conical cambered leading edge and a 10° upward reflex of the wing trailing edge outboard of the elevons. In conjunction with this modification, additional wing fences were installed at the 37-percent wing-span station, and the outboard fences were extended around the leading edge of the wing as shown in figure 3.

The flight control surfaces are conventional flap-type controls actuated by an irreversible hydraulic power control system integrated with the pilot's stick and rudder pedals through a "q-sensitive" type artificial-feel system. The longitudinal-feel system was designed to present the pilot with a relatively constant stick-force gradient over the operational speed and altitude range of the airplane.

During the flight investigation no pitch or yaw dampers were installed in the airplane.

The mass and geometric characteristics of the airplane as obtained from the manufacturer are presented in table I.

INSTRUMENTATION

The airplane was equipped with standard NACA instrumentation to record the following quantities pertinent to the stability and control investigation:

Airspeed and altitude
Angles of attack and sideslip
Normal and transverse accelerations
Pitch, roll, and yawing velocities and accelerations
Control stick and rudder pedal positions
Elevator, aileron, and rudder positions
Elevator, aileron, and rudder forces

A 1/10-second timer was used to correlate all instruments.

The airspeed head, angle-of-attack and angle-of-sideslip vanes were mounted on a boom extending forward of the airplane nose. The static pressure and total pressure orifices on the airspeed head are located at points 79 inches and 87 inches, respectively, ahead of the fuselage zero station. The airspeed installation was calibrated by the radar phototherodolite method, and the Mach number is believed accurate to ± 0.01 .

The angle of attack, measured by a vane approximately 64 inches forward of the fuselage zero station, is corrected for errors introduced by boom bending and pitching velocity. No attempt was made to correct errors resulting from vane floating or upwash.

The airplane weight was determined from the fuel-quantity-gage readings recorded by the pilot at the beginning of each maneuver and is considered accurate to ± 100 pounds.

TESTS

Initially the test program was conducted with the symmetrical-wing configuration; however, after several flights were completed, the wing was modified to the present cambered version. As a result, only trim data are presented for the symmetrical-wing configuration and the remaining portion of the data is for the cambered wing.

The longitudinal stability and trim characteristics of the airplane were determined over the Mach number range of 0.60 to 1.18 during wind-up turns, level-flight speed runs, shallow dives, and elevator pulses. The low-speed characteristics of the airplane were determined from stall approach maneuvers where the speed reduced to $M = 0.32$. The original program was planned to investigate the drag and stability at test altitudes of 25,000 and 40,000 feet; however, the airplane was restricted structurally to a normal load factor of 3.7g. Consequently, to extend the lift-coefficient range of the investigation without exceeding this g restriction, additional maneuvers were performed at 50,000 feet.



At Mach numbers above $M = 0.90$ at altitudes of 40,000 and 50,000 feet, while attempting to hold constant airspeed, a considerable loss in altitude was encountered during a particular maneuver. Therefore, the specified altitude is the initial altitude at which the maneuver was performed.

The center-of-gravity location varied from 28.75 to 29.40 percent of the mean aerodynamic chord for the symmetrical-wing configuration. The modification of the wing to the cambered-wing configuration shifted the center of gravity forward, and the consequent variation ranged from 28.25 to 29 percent of the mean aerodynamic chord.

RESULTS AND DISCUSSION

Longitudinal Trim

The longitudinal stick-fixed trim variation with Mach number at 1 g, 2g, and 3g is presented in figures 4 and 5 for the cambered- and symmetrical-wing configurations, respectively. These data cover the speed range from $M = 0.32$ to $M = 1.18$ and are corrected to altitudes of 25,000, 40,000, and 50,000 feet. It was determined that the small movement of the center of gravity had a negligible effect during these tests.

The data between $M = 0.60$ and $M = 1.18$, used to establish the 1 g trim curves, were obtained from speed runs, while the low-speed portion of the 1 g curve from $M = 0.32$ to $M = 0.60$ was obtained from the gear-up stall approach maneuver of figure 7(a). The 2g and 3g data were obtained during wind-up turns performed at essentially constant Mach number. The faired curves shown for these advanced g levels were computed by assuming a constant control effectiveness through the lift range and using the corresponding 1 g trim curve in conjunction with a variation of $d\delta_e/d\alpha_n$ with Mach number obtained from wind-up turns at the specified altitude. It is realized that nonlinearities exist in the variation of δ_e with C_{N_A} ; however, in the region where these calculations were made these nonlinearities were not appreciable. Figure 4 shows good agreement between the computed curves and the data points for the 2g and 3g levels, with the exception of the 3g data of figure 4(b).

The variation with Mach number of the elevator required for 1 g trim for both the cambered and symmetrical wing appears conventional in the transonic region. From the 1 g condition presented for the cambered wing in figure 4, the trim-change region generally occurs above $M = 0.87$. In this region, the data at 25,000 and 40,000 feet show that the unstable condition exists generally between $M = 0.87$ and $M = 0.95$.

However, the extended supersonic data of figure 4(b) indicate that an additional instability occurs above $M = 1.04$. At the test altitude of 50,000 feet, the unstable portion occurs above $M = 0.87$ and does not indicate a tendency to become stable within the region tested (up to $M = 0.98$). A comparison of this unstable region for the three test altitudes indicates that the instability becomes more pronounced with increasing altitude.

An observed deviation from the normal trim variation was experienced with the symmetrical wing at an altitude of 40,000 feet, as shown in figure 5(b). With this configuration at the specified altitude there was a region of scatter in the data of 1.0° to 1.6° , indicating that there was no unique variation of elevator for trim throughout the Mach number range. Figure 6(a) shows that the symmetrical-wing trim data are similar to the cambered-wing data, with only a change in level constituting the difference. At 25,000 feet the cambered-wing modification appears to have reduced the trim elevator by approximately 0.6° to 1.9° over the Mach number range from the trim setting required with the symmetrical wing.

The variation of 1 g stick-free static stability with Mach number is presented in figure 6(b) and generally follows the trend defined by the stick-fixed presentation. The main difference is that the stick force at 50,000 feet appears to be less than at 40,000 feet between $M = 0.90$ and $M = 0.97$. This difference is probably the result of the initial trim setting in conjunction with the artificial-feel system operation.

The investigation was extended to obtain pilot opinion on the handling qualities of the airplane while flying for periods of 4 minutes in the stable region ($M = 0.75$), neutrally stable region ($M = 0.88$ and 1.04), and unstable region ($M = 0.93$) of the 1 g trim curve. This was accomplished by making steady constant-speed, level runs at 40,000 feet. The data did not indicate any adverse handling difficulties and the pilot commented that the airplane handled satisfactorily. He did state, however, that considerably more attention and control manipulation was required to handle the airplane at $M = 0.93$ than was necessary at the other speeds. This would be expected since $M = 0.93$ is in the unstable trim region. The pilot also stated that, although he was aware of the trim change, he experienced no appreciable handling difficulties while accelerating or decelerating through the trim-change region.

Stall Maneuvers

Figure 7 presents representative time histories of gear-up and gear-down stall approach maneuvers performed at an altitude of 25,000 feet. From a comparison of these data, it is evident there

is no appreciable difference in the handling qualities exhibited between the gear-up and gear-down configuration. With the gear up, the airplane attained an approximate angle of attack and airspeed of 26.5° and 105 knots, respectively; with the gear down, an angle of attack of 17.0° and an airspeed of 130 knots were attained. The latter stall was terminated at the conditions indicated as a result of the decreased lift-to-drag ratio and increased rate of sink with the gear extended.

Dynamic Longitudinal Stability

The longitudinal period and damping characteristics (fig. 8) were determined by performing elevator pulses at altitudes of 25,000 and 40,000 feet. To investigate the more extreme damping characteristics of the airplane, additional pulses were performed at 10,000 feet and 50,000 feet. From the measured quantities of P and $T_{1/2}$, the cycles to damp to one-half amplitude have been computed for comparison with the Military Specification of reference 2. A comparison is also made on the basis of damping to one-tenth amplitude in 1 cycle. The $C_{1/2}$ and $C_{1/10}$ variations with period (fig. 8) indicate that, although the airplane will not damp to one-tenth amplitude in 1 cycle, it does meet the Military Specification. Generally, the pilots commented that the longitudinal damping was insufficient, which indicates that the Specification is inadequate for this airplane.

Maneuvering Stability

The maneuvering stability over the attainable Mach number and lift-coefficient range of the YF-102 airplane was investigated by performing wind-up turns at altitudes of 25,000, 40,000, and 50,000 feet. Figures 9(a) to 9(c) are typical time histories of turns initiated at $M \approx 0.70$, $M \approx 0.89$, and $M \approx 1.13$ at 40,000 feet. At $M \approx 0.70$ maximum values of $C_{NA} = 0.62$ and $\alpha \approx 17.5^\circ$ were reached. To extend the C_{NA} and α range, turns were performed at an altitude of 50,000 feet. Figure 9(d) is a typical time history of a turn initiated at $M = 0.93$ at 50,000 feet where the C_{NA} and α reached approximately 0.78 and 21.5° , respectively.

Upon analyzing the data and reviewing the pilot's comments, it was apparent that there was no well-defined pitch-up exhibited throughout the speed and altitude range tested. However, the data, typified by the plots of the maneuvering stability characteristics of figure 10 for the time histories of figure 9, indicated a slight decrease in the longitudinal stability at the higher values of g and angles of attack.

The variation of stick forces presented in figure 10 shows an instability not indicated by the variation of elevator position with angle of attack. This indication of instability is felt to be a function of the artificial-feel system operation. The nonlinearities in the pitching-moment curves (fig. 10) computed by using the expression

$$C_m = \frac{I_y \dot{q}}{\frac{1}{2} \rho v^2 S \bar{c}} - C_{m\delta_e} \Delta \delta_e$$

are felt to result partially from the nonlinear derivative $C_{m\delta_e}$ and from the control input during the maneuver.

An inspection of figure 9(d) might, at first, indicate a slight pitch-up between $t = 8.2$ and 10 seconds. During this time, C_{N_A} increased from 0.48 to 0.72, while the longitudinal stick force and the elevator control surface remained essentially fixed at approximately 22 pounds and 10° , respectively. By observing figure 4(c), it is apparent the maneuver was performed in the trim change region where a loss in speed without a corresponding reduction of δ_e results in an untrimmed condition. Consequently, in this case, with the controls remaining fixed and a decrease in speed from $M = 0.92$ to $M = 0.89$, the rapid increase in C_{N_A} can be attributed to the induced pitching moment resulting from the out-of-trim elevator deflection. The investigation of the longitudinal handling qualities was extended to determine the pilot's ability to control the airplane in the trim-change region at the 2g and 3g levels while the speed rapidly decreased. Figure 11 is a time history of one of these maneuvers in which the pilot attempted to maintain approximately 2g and a constant altitude of 40,000 feet. To decelerate rapidly, the afterburner was turned off upon attaining the desired test conditions at 2g. At $t = 20$ seconds, the airplane experienced a nose-up rotation from the out-of-trim elevator. However, the degree of instability was somewhat obscured from the pilot by the lateral oscillation encountered simultaneously. The pilot felt that the nose-up instability was controllable, but would make tracking another airplane in this speed range difficult. The oscillatory condition encountered is evident over the major operating range of the airplane and considerably hinders the pilot in carrying out the intended mission.

Stability and Control Effectiveness Parameters

Figures 12 and 13 present the variation of the stability and control effectiveness parameters $C_{m\alpha}$, $C_{m\delta_e}$, $C_{N_{A\alpha}}$, $\frac{d\delta_e}{dC_{N_A}}$, and $\frac{dC_m}{dC_{N_A}}$

over the Mach number range from $M = 0.60$ to $M = 1.16$ for altitudes of 25,000, 40,000, and 50,000 feet. The static stability parameter $C_{m\alpha}$ was computed using the period and damping data of figure 8 and the expression

$$C_{m\alpha} = - \frac{I_Y}{\frac{1}{2}\rho V^2 S \bar{c}} \left[\left(\frac{2\pi}{P} \right)^2 + \left(\frac{0.693}{T_{1/2}} \right)^2 \right]$$

The apparent stability parameter $d\delta_e/dC_{N_A}$ shown in figure 12(b) was obtained from data in the low-lift region similar to the data presented in figure 10 and the values of the control effectiveness parameter $C_{m\delta_e}$ for constant α (fig. 12(c)) were determined from elevator pulses.

A comparison of the variation of $C_{m\alpha}$ and $d\delta_e/dC_{N_A}$ with Mach number indicates that there is an increase in control effectiveness below $M = 0.90$, as the airplane stability shows a continual increase while the apparent stability remains essentially constant. Above $M = 0.90$, the percentage of increase in airplane stability is considerably less than the increase in apparent stability, indicating a loss of control effectiveness in this region. This trend is substantiated by the $C_{m\delta_e}$ variation of figure 12(c). In the speed range from $M = 0.92$ to 0.95 , there is an abrupt decrease in $C_{m\alpha}$ from -0.008 to -0.006 , which is paralleled by a decrease in $C_{m\delta_e}$ of approximately 34 percent. This loss in control effectiveness in the transonic range is usually anticipated with flap-type controls.

The $C_{N_{A\alpha}}$ variation of figure 13 was obtained from wind-up turn and elevator-pulse data (elevator fixed) and generally shows the same trend. However, the results from the pulse data show an average increase of approximately 35 percent in $C_{N_{A\alpha}}$ over the turn data.

The static margin dC_m/dC_{N_A} , as determined by combining the static stability parameter $C_{m\alpha}$ and $C_{N_{A\alpha}}$ from elevator pulses, shows a rearward movement of the neutral point of approximately 12-percent mean aerodynamic chord between $M = 0.40$ and $M = 1.16$.

Artificial-Feel System

The inconsistency of the stick-fixed and stick-free stability characteristics typified by figures 10(a) to 10(d) led to a preliminary investigation of the artificial-feel system.

Primarily, the system provides an artificial-feel force to the pilot's stick through a pneumatically operated cylinder. The pneumatic pressure is obtained from total head probes on the vertical fin and from the engine bleed air duct aft of the compressor. The air from these sources passes through a Mach compensating regulator to the feel force cylinder. The Mach compensating regulator functions according to the variation of the combined vertical fin and engine bleed air total head with compartment static pressure. The compartment static pressure is the pressure measured in an aft compartment of the airplane where the compensator unit is located. Through the regulation of the pneumatic pressure by the Mach compensating unit, the feel cylinder is designed to provide the pilot with a relatively constant stick-force gradient over the operational Mach number and altitude range.

At the onset of the investigation, a ground calibration of the feel system was made to check the system performance with that specified by the manufacturer. Figure 14 presents the results of the calibration in conjunction with comparable flight data obtained for the Mach number range from $M = 0.75$ to $M = 1.18$ at 40,000 feet. The calibration results indicate that the compensating unit is functioning on the ground according to specification. However, an inspection of the flight data shows that at altitude, between $M = 0.85$ and $M = 1.18$, the operating pressure ratio P_3/P_1 for the Mach compensating unit is increased appreciably above that specified by design.

The variation of F_e/δ_e with Mach number obtained during the ground calibration was extrapolated to the test altitude and converted to F_e/a_n by using the flight-determined δ_e/a_n . As shown in figure 15, the feel system meets the requirements of the Military Specification. For these conditions a constant F_e/a_n of approximately 6 pounds per g would be supplied over the speed range. However, the flight-measured F_e/a_n exceeds the specification by as much as 100 percent, indicating that the system is not functioning in the air as it does on the ground. From figure 14 it appears that the improper regulation of the pneumatic pressure to the feel cylinder may be the cause of the objectionably high force gradient experienced between $M = 0.90$ and 1.10. The improper pressure regulation by the compensating unit is influenced by several features inherent in the feel system installation. Primarily, the total head probe on the vertical fin is located in a position where it will be greatly influenced by the variation of the flow field with changing

angle of attack. Secondly, use of the compartment static pressure as a reference pressure for the unit may be improper since the compartment is vented through a cooling duct, which results in the compartment pressure being subject to changing boundary-layer conditions. Also, the engine compressor air being fed into the Mach compensating instrument has a tendency to leak into the static pressure side of the instrument and thus influences the static reference. It is felt these features contribute directly to the poor stick-free stability characteristics exhibited in figure 10.

As a result of this preliminary analysis, a minor modification was made to supply the Mach compensating unit with a static reference from the nose boom. Figure 16 presents a comparison of the data obtained with and without the new static source at $M \approx 0.95$ at 50,000 feet. It is apparent from the data that the modification had no appreciable effect on the feel characteristics. However, it was realized after the tests were made that the effect of the leakage of engine bleed air into the static pressure side of the compensating instrument was sufficient to nullify any improvements which might be expected with the modification.

Generally, the pilots commented that the force gradient at the lower Mach numbers was low and they seriously objected to the high forces experienced in the transonic region.

CONCLUSIONS

The following conclusions may be made in conjunction with the analysis of the longitudinal stability data obtained during the flight investigation of the cambered-wing configuration of the YF-102 airplane:

1. The variation of elevon trim required over the Mach number range appears to be conventional, with the unstable region occurring generally between Mach numbers of 0.87 and 0.95. The degree of instability in this region becomes more pronounced with increasing altitude. At 40,000 feet the conventional trim change was followed by a marked nose-up trim change which occurred above a Mach number of 1.04. There were no adverse handling difficulties experienced while accelerating or decelerating through the trim-change region; however, sustained flight in the unstable trim region required above average effort.
2. A comparison of the cambered and symmetrical wing 1 g trim data showed the cambered-wing modification reduced the elevator required for trim by approximately 0.6° to 1.9° at 25,000 feet.
3. The longitudinal damping characteristics meet the Military Specification of damping to one-half amplitude in 1 cycle and indicate

that damping to one-tenth amplitude in 1 cycle could not be attained. Generally, the pilots commented that the damping was insufficient.

4. Although a gradual decrease in stability with increase in lift was noted during accelerated maneuvers at constant Mach number, no severe pitch-up tendencies were exhibited by the airplane except possibly during maneuvers involving rapid speed loss in the transonic trim-change region.

5. Generally, the stability more than doubles between a Mach number of 0.60 and a Mach number of 1.16. The control effectiveness, however, shows an increase up to a Mach number of approximately 0.89 with a rapid decrease of approximately 50 percent occurring between Mach numbers of 0.90 and 1.0.

6. An abrupt decrease in the force gradient generally occurring between 1.5g and 2.0g is felt to be caused primarily by the location of the total head probe for the Mach compensating instrument of the artificial-feel system.

7. The poor regulation of the pneumatic pressure to the feel cylinder of the artificial-feel system constitutes an objectionable increase in the stick-force gradient in the transonic region.

High-Speed Flight Station,
National Advisory Committee for Aeronautics,
Edwards, Calif., August 27, 1956.

REFERENCES

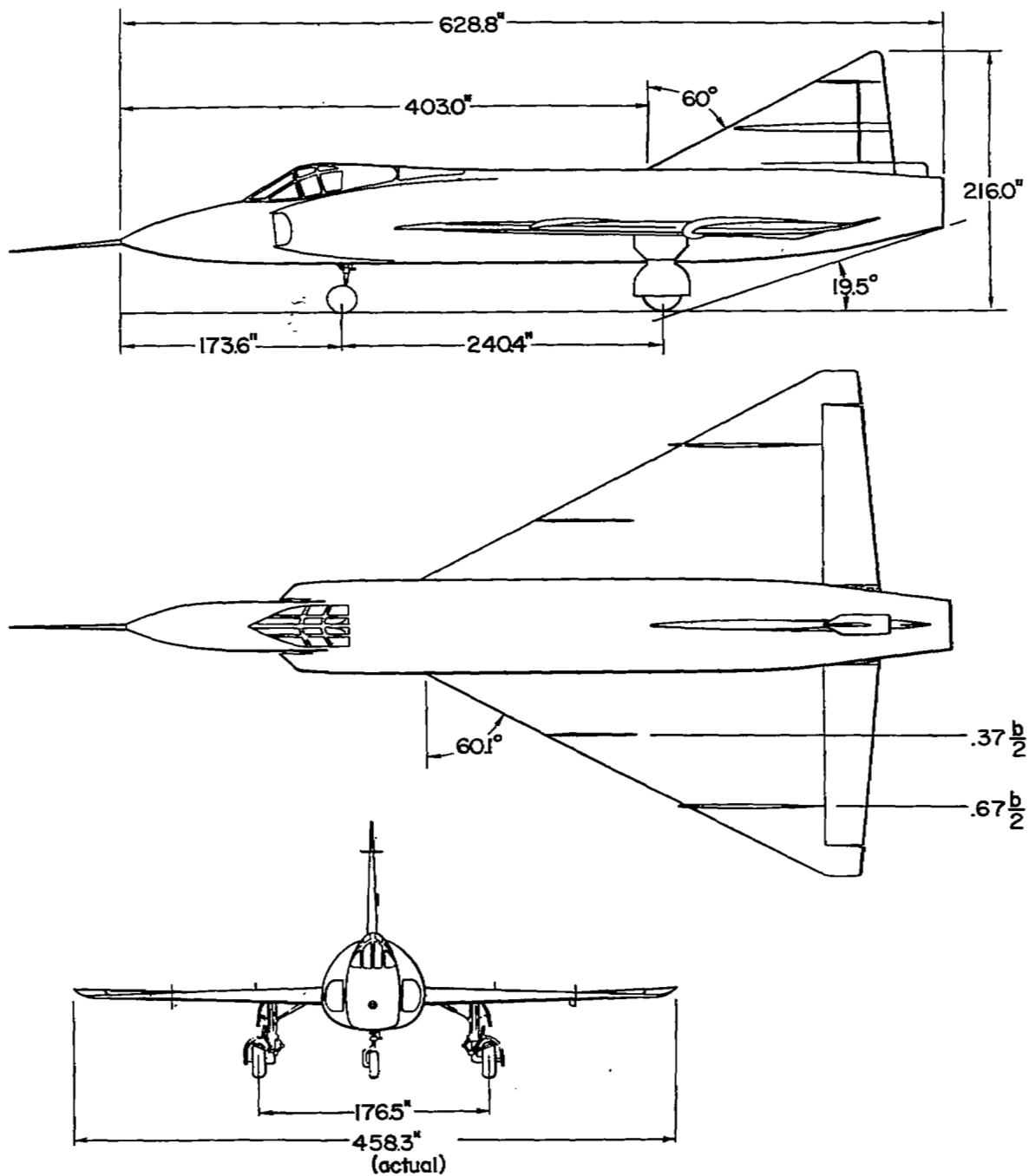
1. Saltzman, Edwin J., Bellman, Donald R., and Musialowski, Norman T.: Flight-Determined Transonic Lift and Drag Characteristics of the YF-102 Airplane With Two Wing Configurations. NACA RM H56E08, 1956.
2. Anon: Military Specification - Flying Qualities of Piloted Airplanes. MIL-F-8785 (ASG), 1 September 1954.

TABLE I.- PHYSICAL CHARACTERISTICS OF THE YF-102 AIRPLANE

	Cambered	Symmetrical
Wing:		
Airfoil section	NACA 0004-65 (modified)	NACA 0004-65 (modified)
Total area, sq ft	695.05	661.50
Span, ft	38.19	37.03
Mean aerodynamic chord, ft	23.75	23.13
Root chord, ft	35.63	34.69
Tip chord, ft	0.81	0
Taper ratio	0.023	0
Aspect ratio	2.08	2.20
Sweep at leading edge, deg	60.6	60
Incidence, deg	0	0
Dihedral, deg	0	0
Conical camber (leading edge), percent chord	6.3	None
Geometric twist, deg	0	0
Inboard fence, percent wing span	37	None
Outboard fence, percent wing span	67	67
Tip reflex, deg	10	0
Maximum thickness:		
Root, percent chord	3.9	4.0
Outboard edge of elevon, percent chord	3.5	4.0
Elevons:		
Area (total, both rearward of hinge line), sq ft	67.77	67.77
Span (one elevon), ft	13.26	13.26
Root chord (rearward of hinge line) parallel to fuselage center line, ft	3.15	3.15
Tip chord (rearward of hinge line), ft	2.03	2.03
Elevator travel, deg:		
Up	35	35
Down	20	20
Aileron travel, total, deg	20	20
Operation	Hydraulic	Hydraulic
Vertical tail:		
Airfoil section	NACA 0004-65 (modified)	
Area (above waterline 33), sq ft	68.33	
Sweep at leading edge, deg	60	
Height above fuselage center line, ft	11.41	

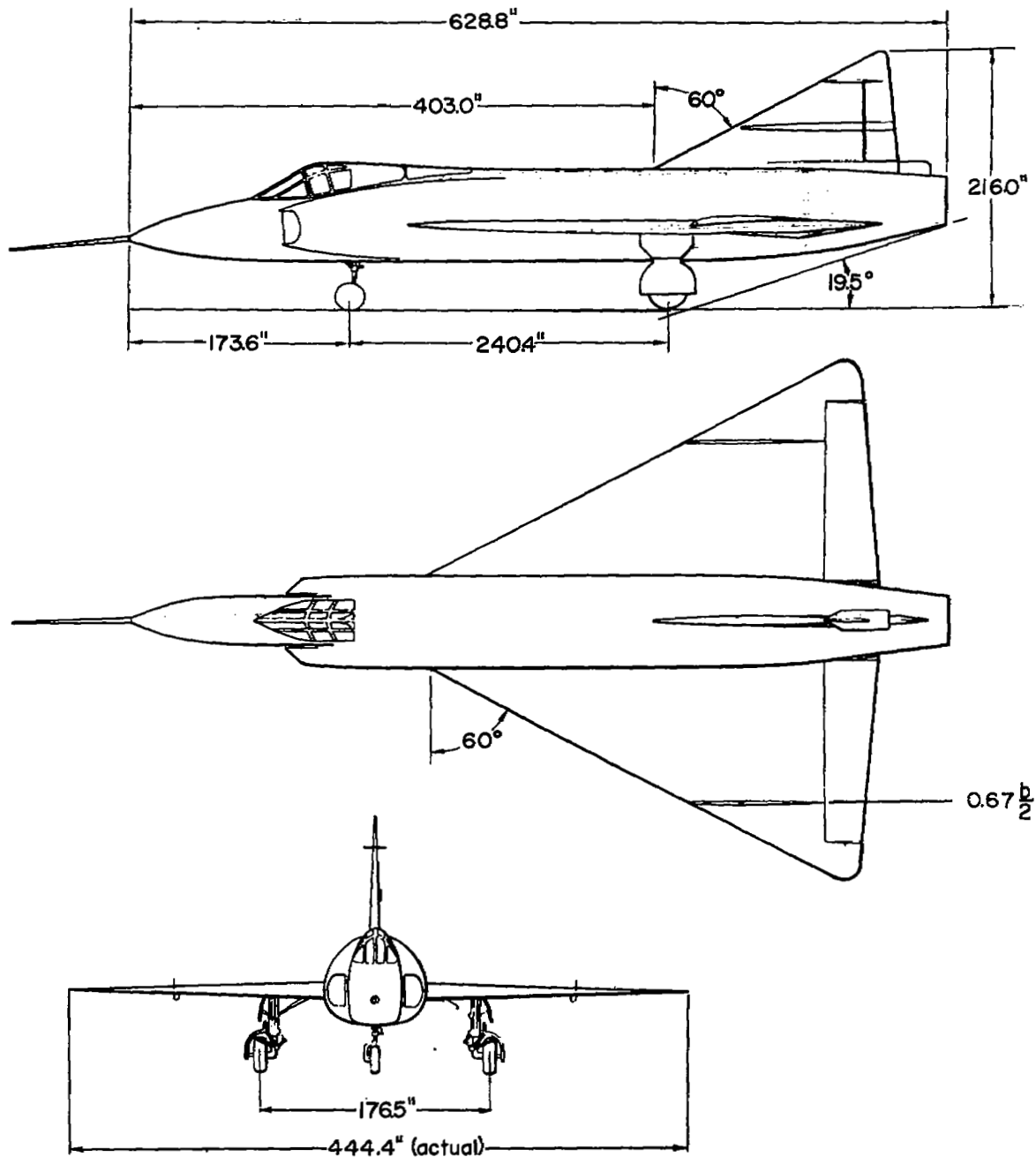
TABLE I.- PHYSICAL CHARACTERISTICS OF THE YF-102 AIRPLANE - Concluded

Rudder:	
Area (rearward of hinge line), sq ft	10.47
Span, ft	5.63
Root chord (rearward of hinge line), ft	2.10
Tip chord (rearward of hinge line), ft	1.61
Travel, deg	+25
Operation	Hydraulic
Fuselage:	
Length, ft	52.4
Maximum diameter, ft	6.5
Power plant:	
Pratt & Whitney	J57-P11 turbojet engine with afterburner
Static thrust at sea level, lb	9,700
Static thrust at sea level, afterburner, lb	14,800
Weight:	
Empty, lb	21,235
Total (1,010 gal fuel at 6.5 lb per gal), lb	27,800
Center-of-gravity location, percent \bar{c} :	
Empty weight	25.6
Total weight	29.8
Moments of inertia (estimated for 24,000 lb gross weight):	
I_x , slug-ft ²	13,200
I_y , slug-ft ²	106,000
I_z , slug-ft ²	114,600
I_{xz} , slug-ft ²	3,540
Inclination of principal axis (estimated) below reference axis at nose, deg	
	2



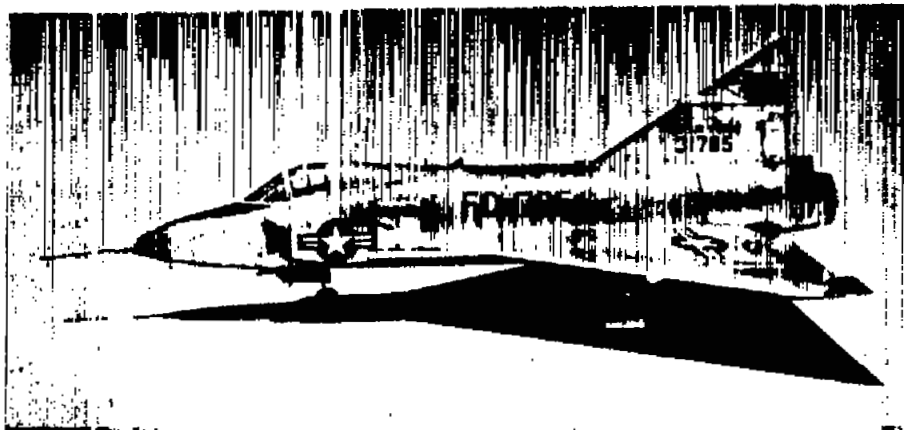
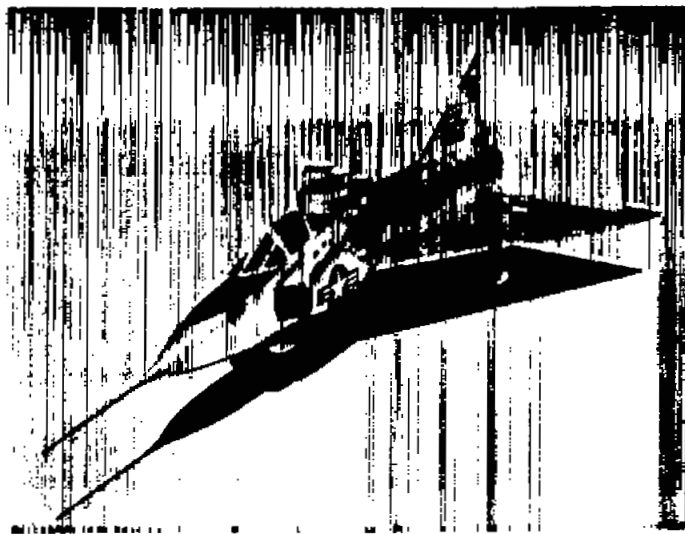
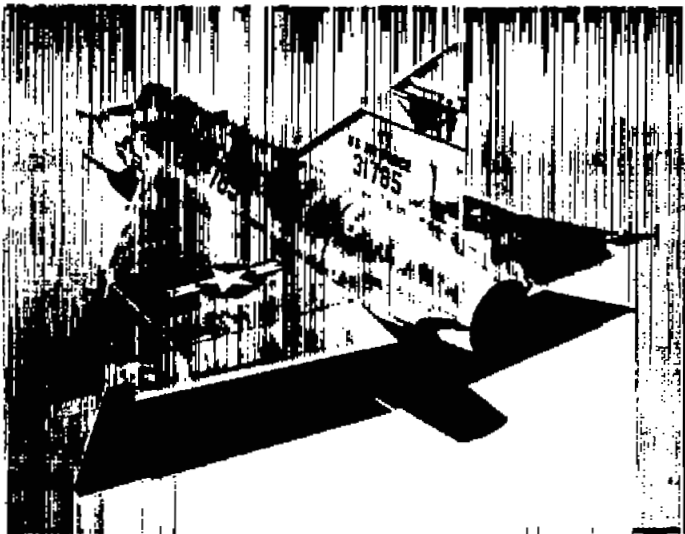
(a) Cambered-wing configuration.

Figure 1.- Three-view drawings of the YF-102 airplane.



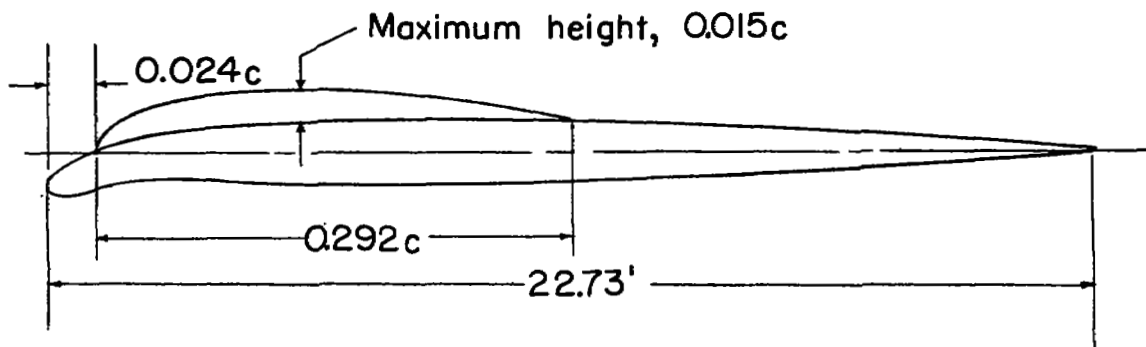
(b) Symmetrical-wing configuration.

Figure 1.- Concluded.

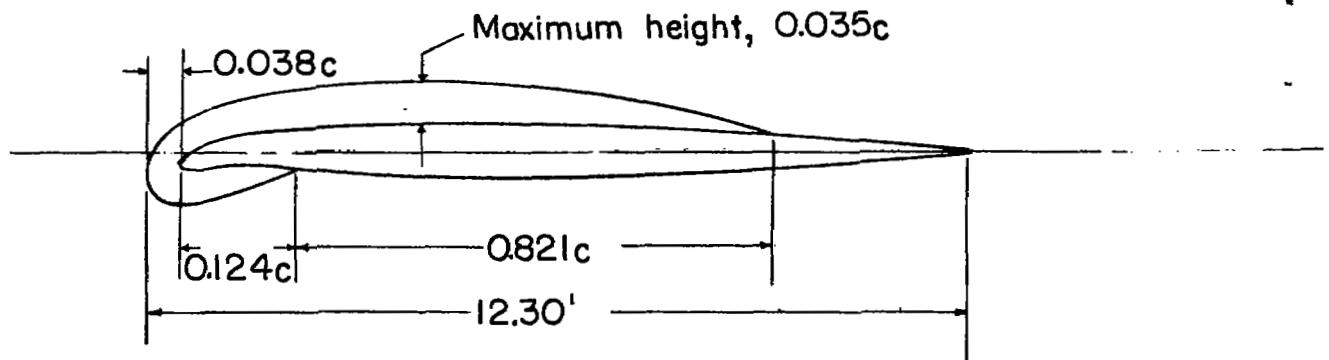


E 1838

Figure 2.- Photographs of the YF-102 airplane with cambered wing.

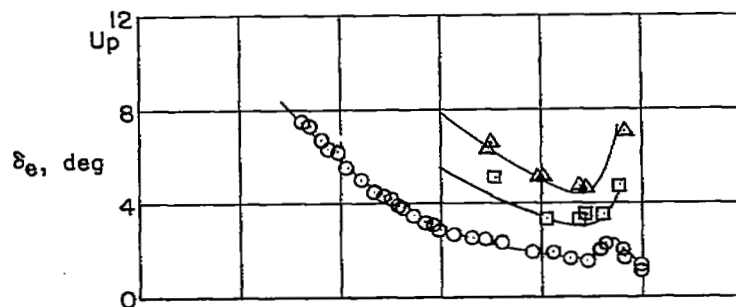


(a) Inboard fence, station $0.37\frac{b}{2}$.

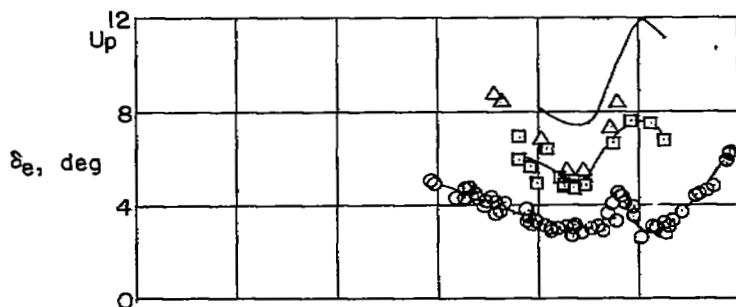


(b) Outboard fence, station $0.67\frac{b}{2}$.

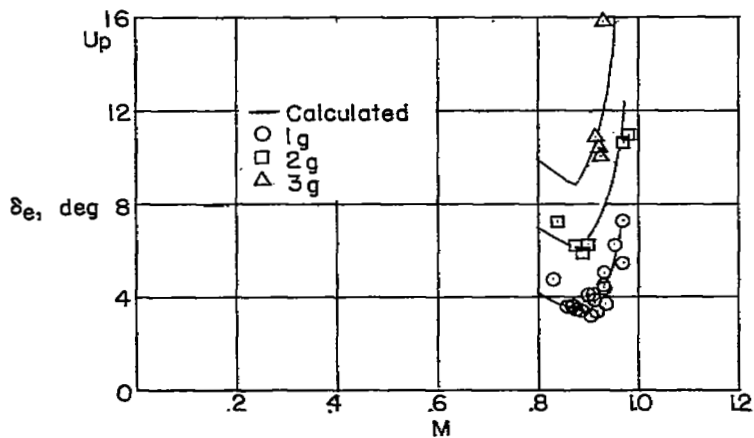
Figure 3.- Sketch of the wing fences for the cambered-wing configuration.



(a) $h_p = 25,000$ feet.



(b) $h_p = 40,000$ feet.



(c) $h_p = 50,000$ feet.

Figure 4.- Elevator required for trim at altitudes of 25,000, 40,000, and 50,000 feet with the cambered-wing configuration of the Convair YF-102 airplane.

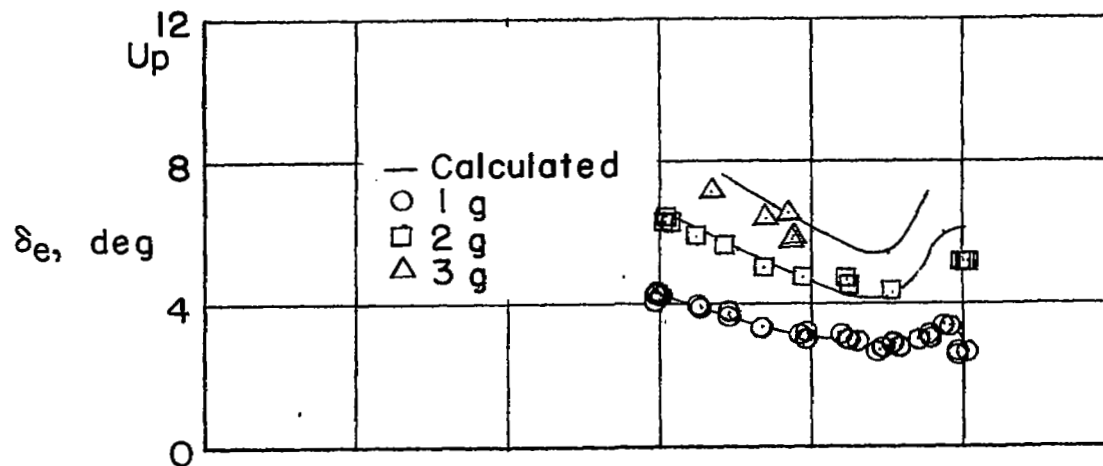
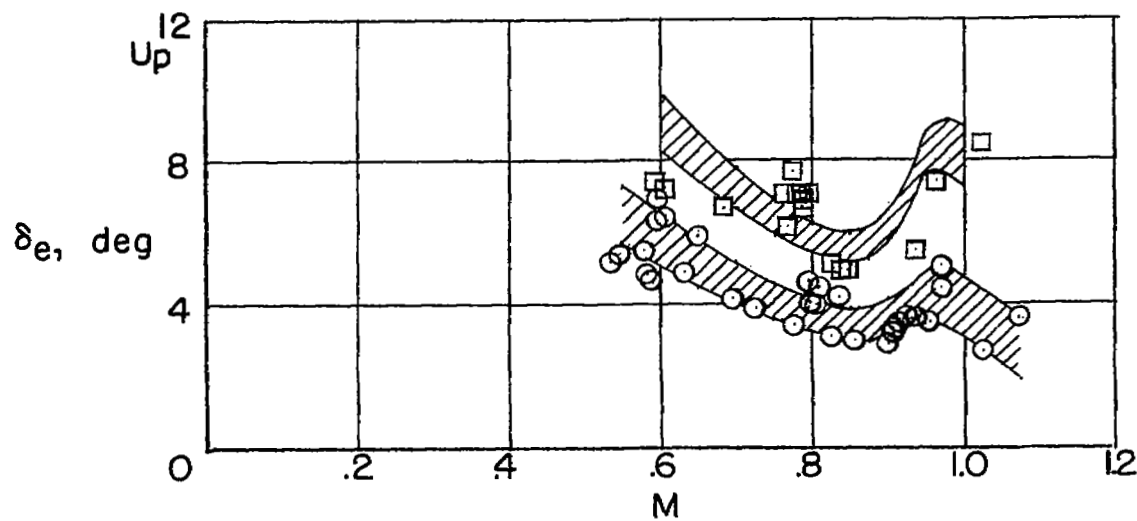
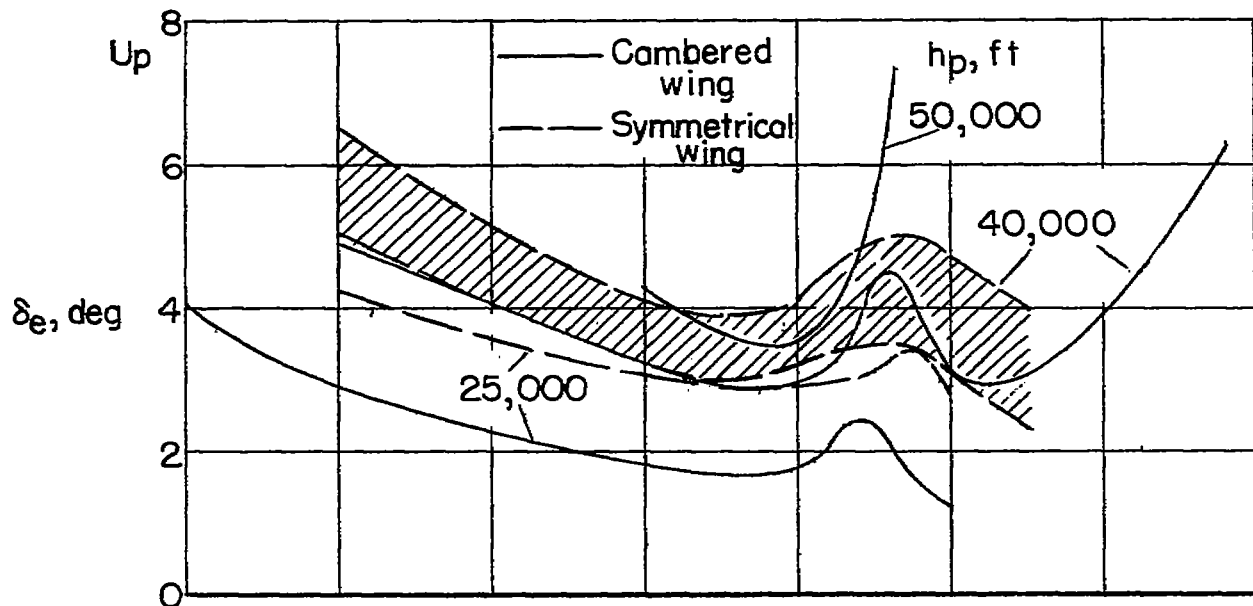
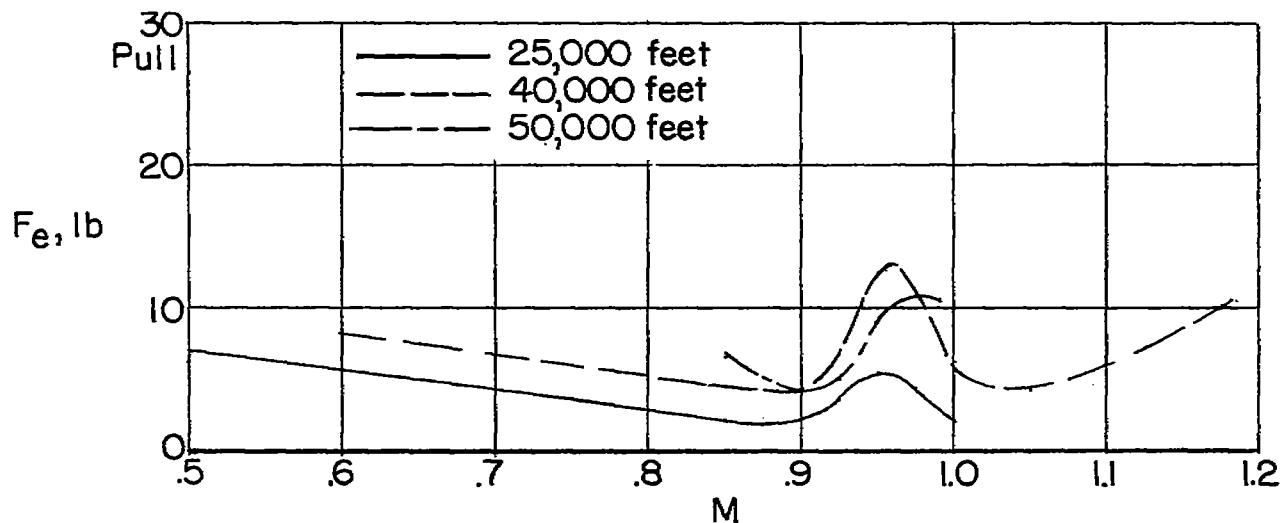
(a) $h_p = 25,000$ feet.(b) $h_p = 40,000$ feet.

Figure 5.- Elevator required for trim at altitudes of 25,000 and 40,000 feet with the symmetrical-wing configuration of the Convair YF-102 airplane.

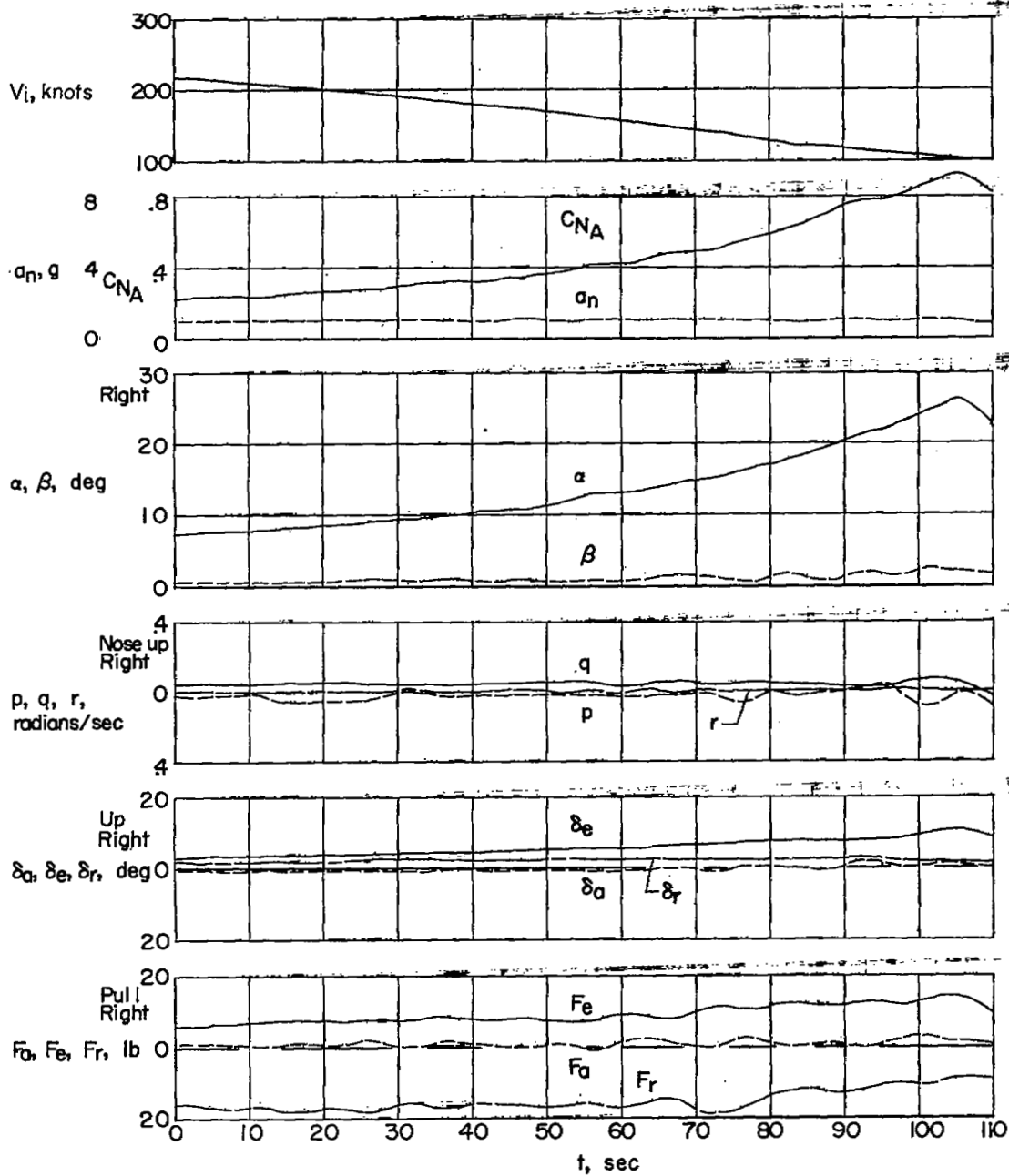


(a) Stick-fixed stability.



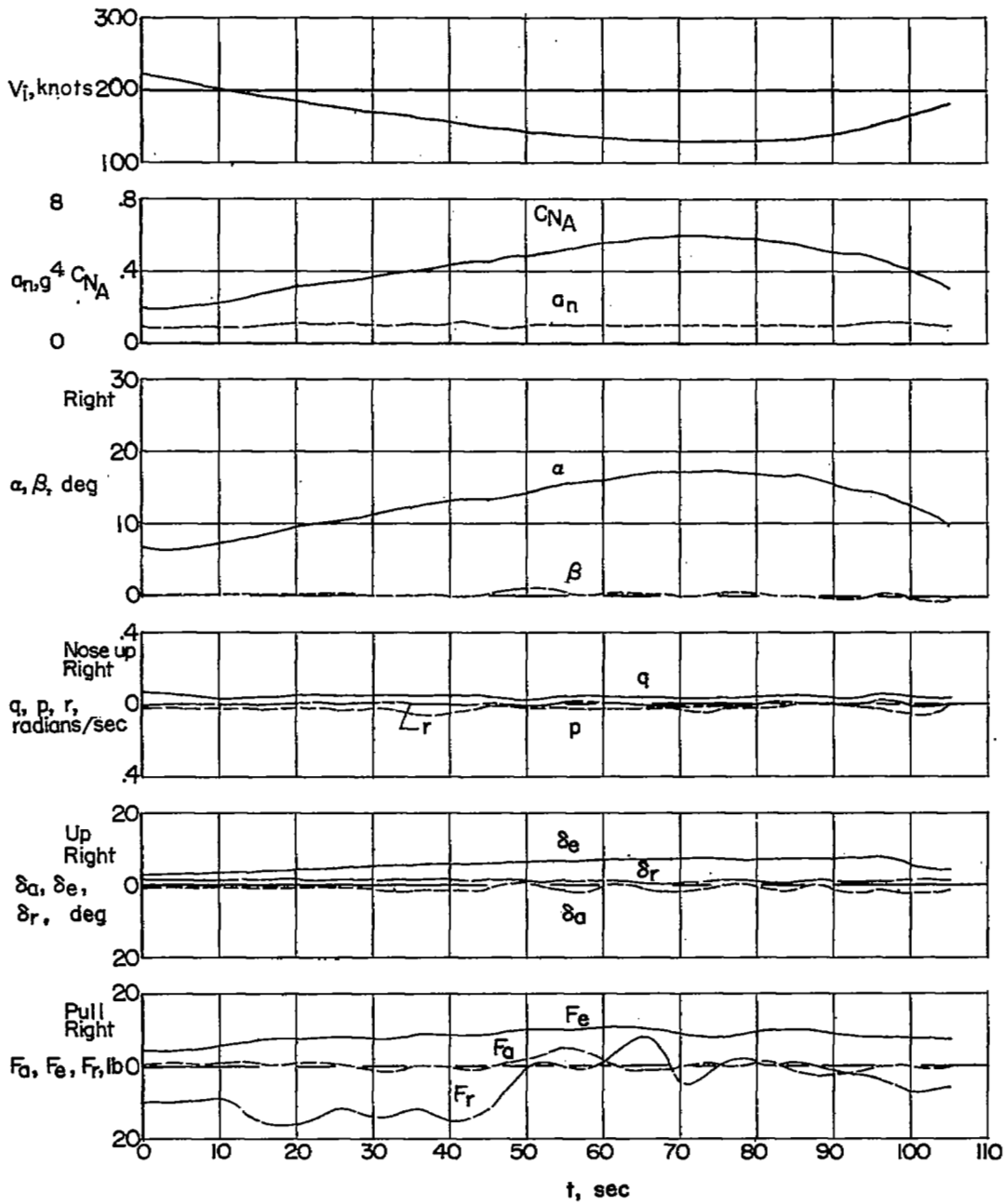
(b) Stick-free stability.

Figure 6.- Stick-fixed and stick-free static stability for the cambered-wing YF-102 airplane at altitudes of 25,000, 40,000, and 50,000 feet.



(a) Gear up; $h_p = 25,000$ feet.

Figure 7.- Typical time histories of stall approach maneuvers with the cambered-wing Convair YF-102 airplane.



(b) Gear down; $h_p = 25,000$ feet.

Figure 7.- Concluded.

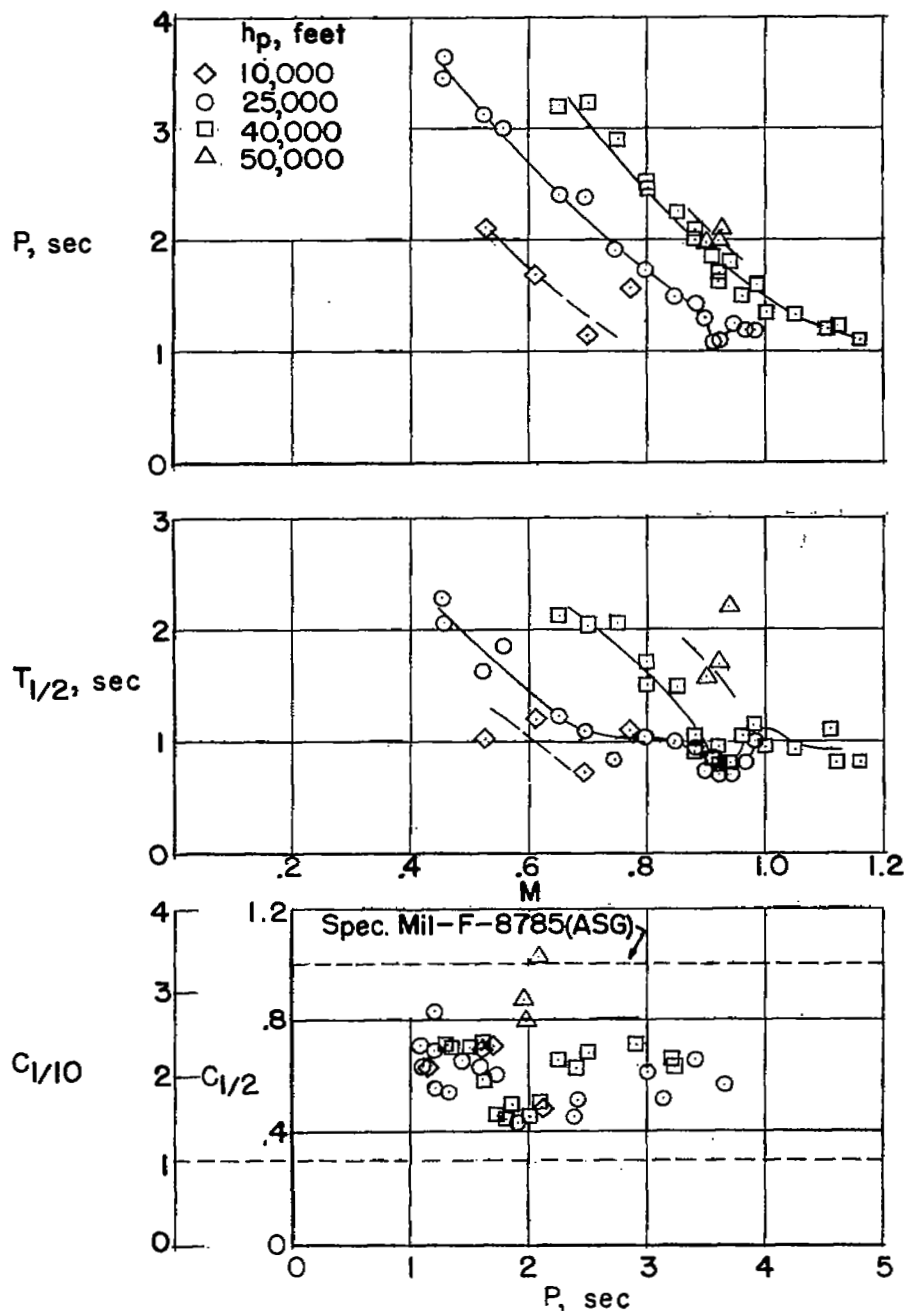
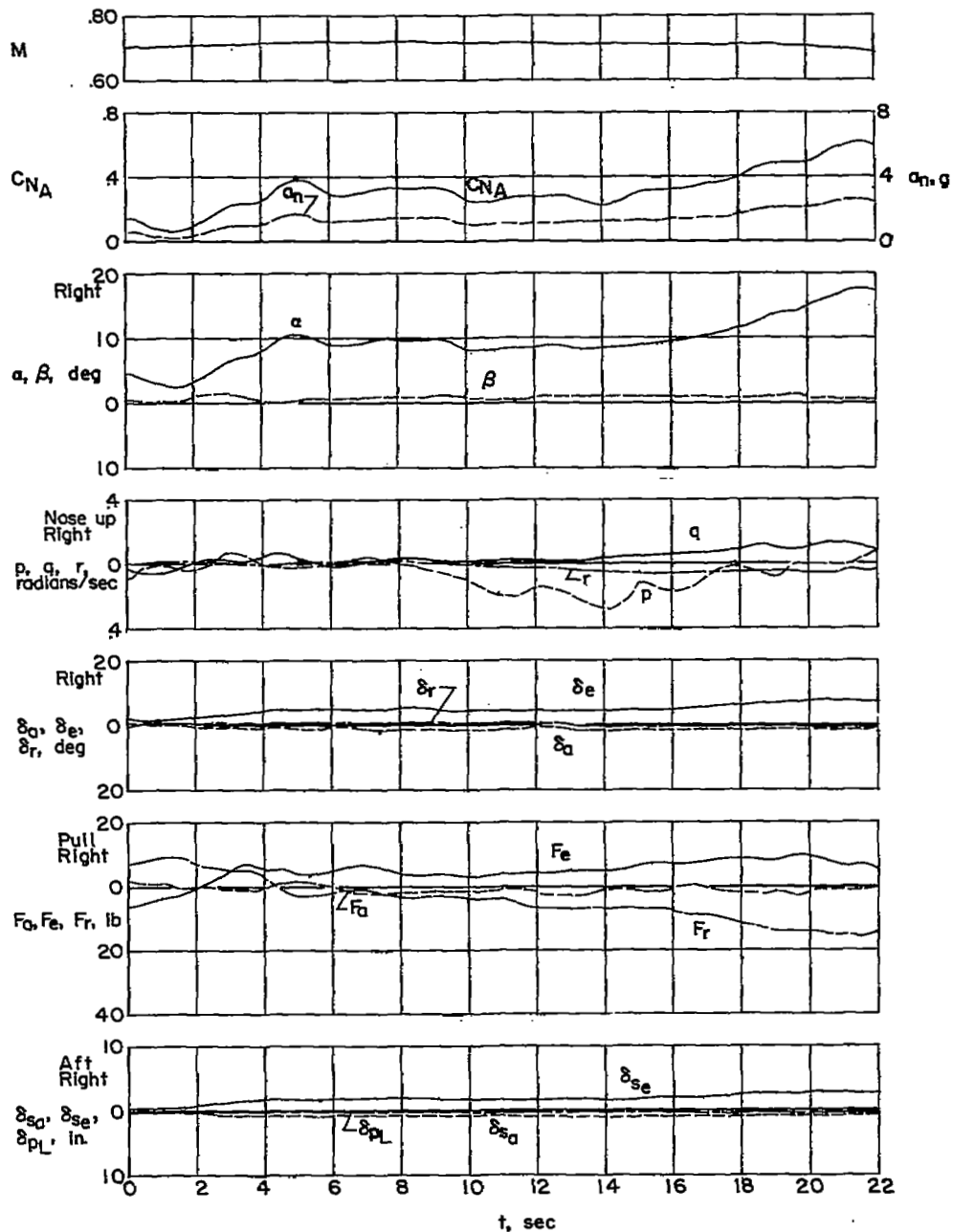
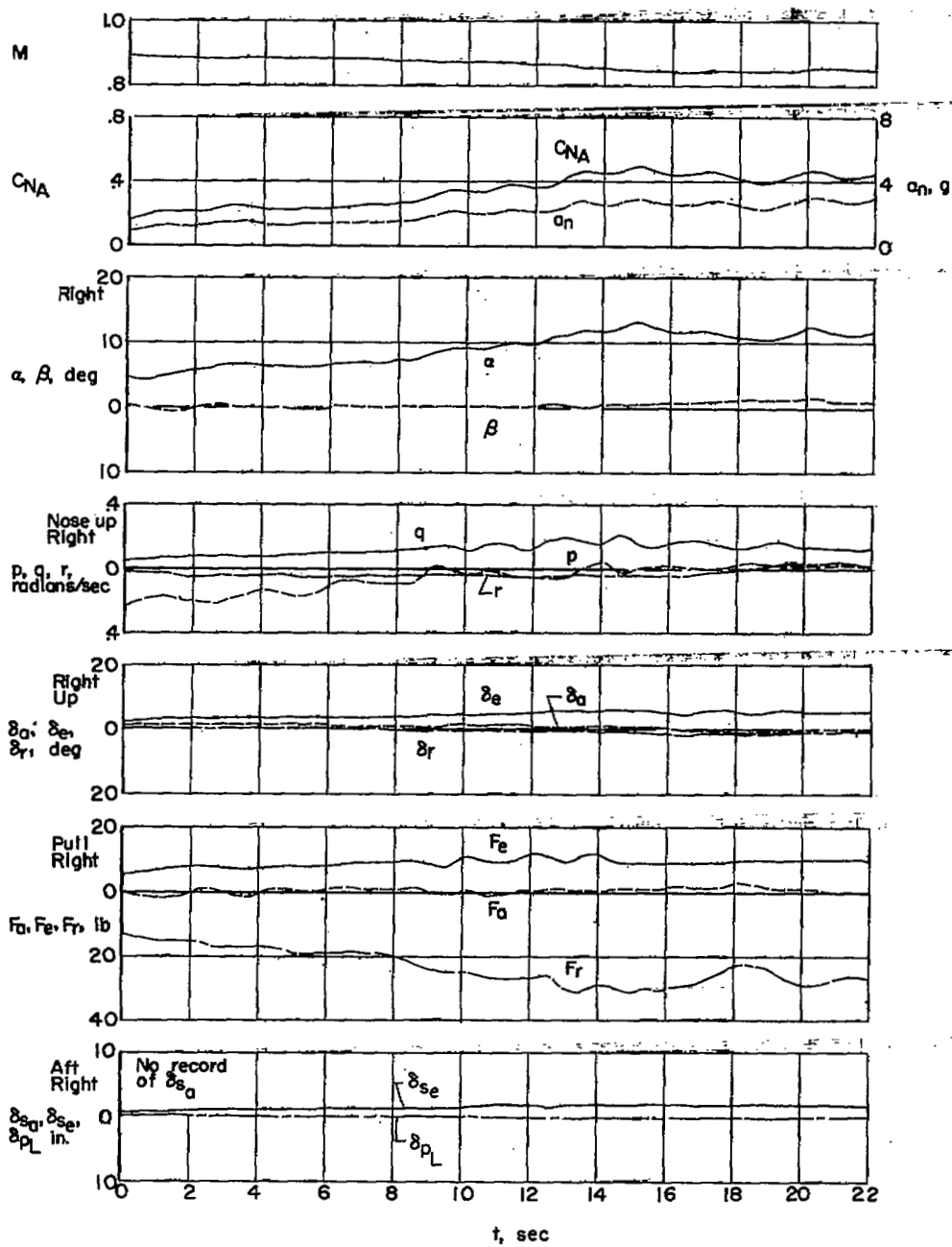


Figure 8.- Variation with Mach number of period and damping characteristics from the longitudinal short-period oscillation. (Cambered-wing configuration.)



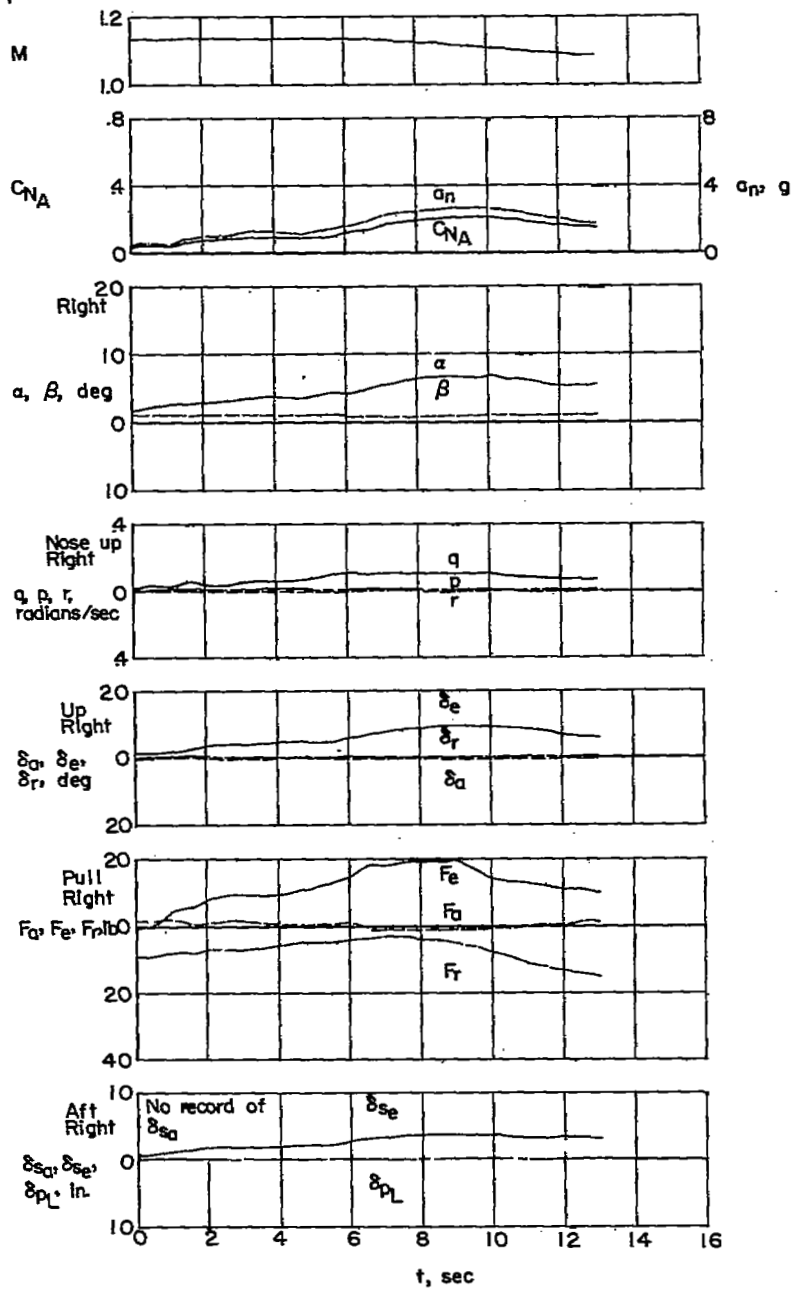
(a) $M \approx 0.70$; $h_p \approx 40,000$ feet.

Figure 9.- Representative time histories of wind-up turns performed with the cambered-wing Convair YF-102 airplane.



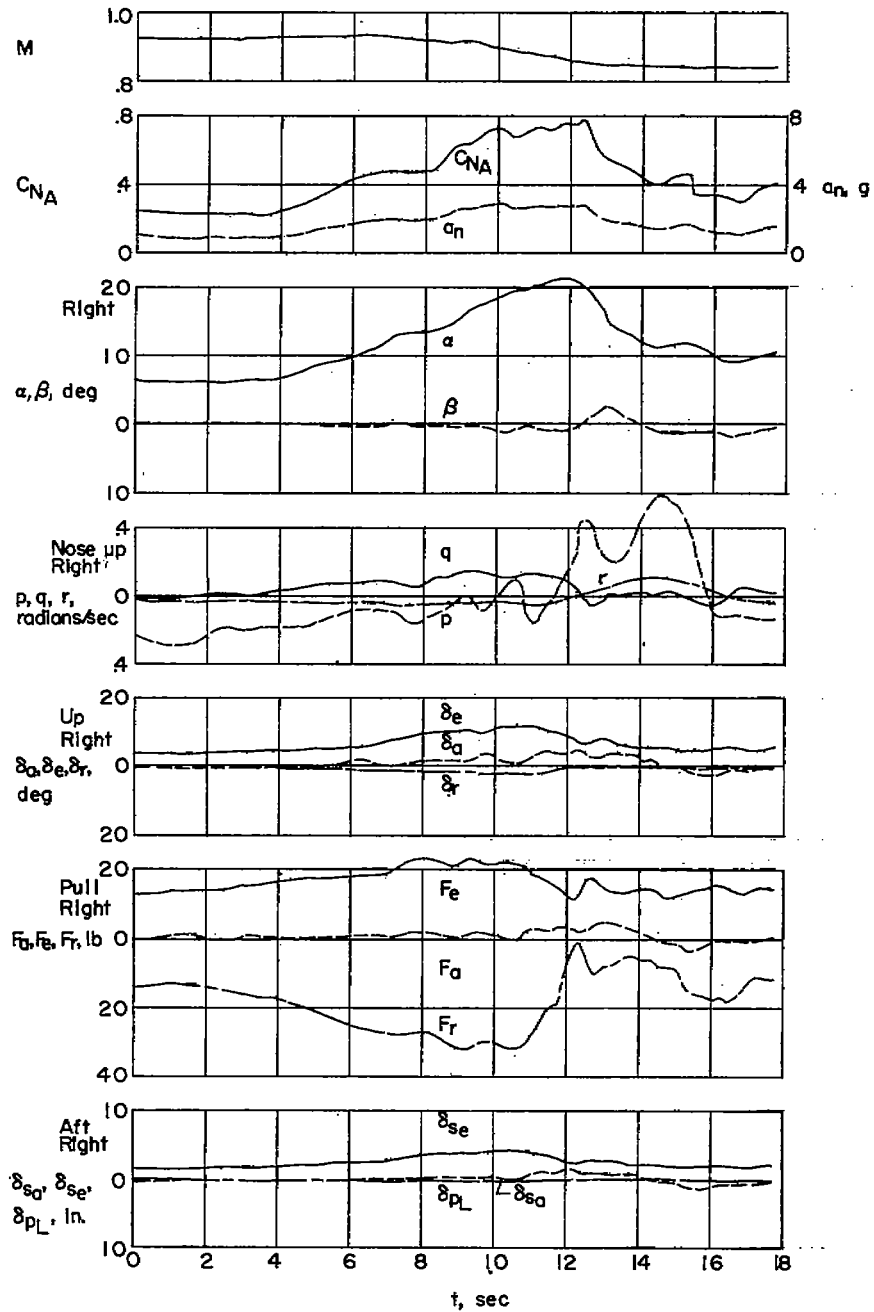
(b) $M \approx 0.89$; $h_p \approx 40,000$ feet.

Figure 9.- Continued.



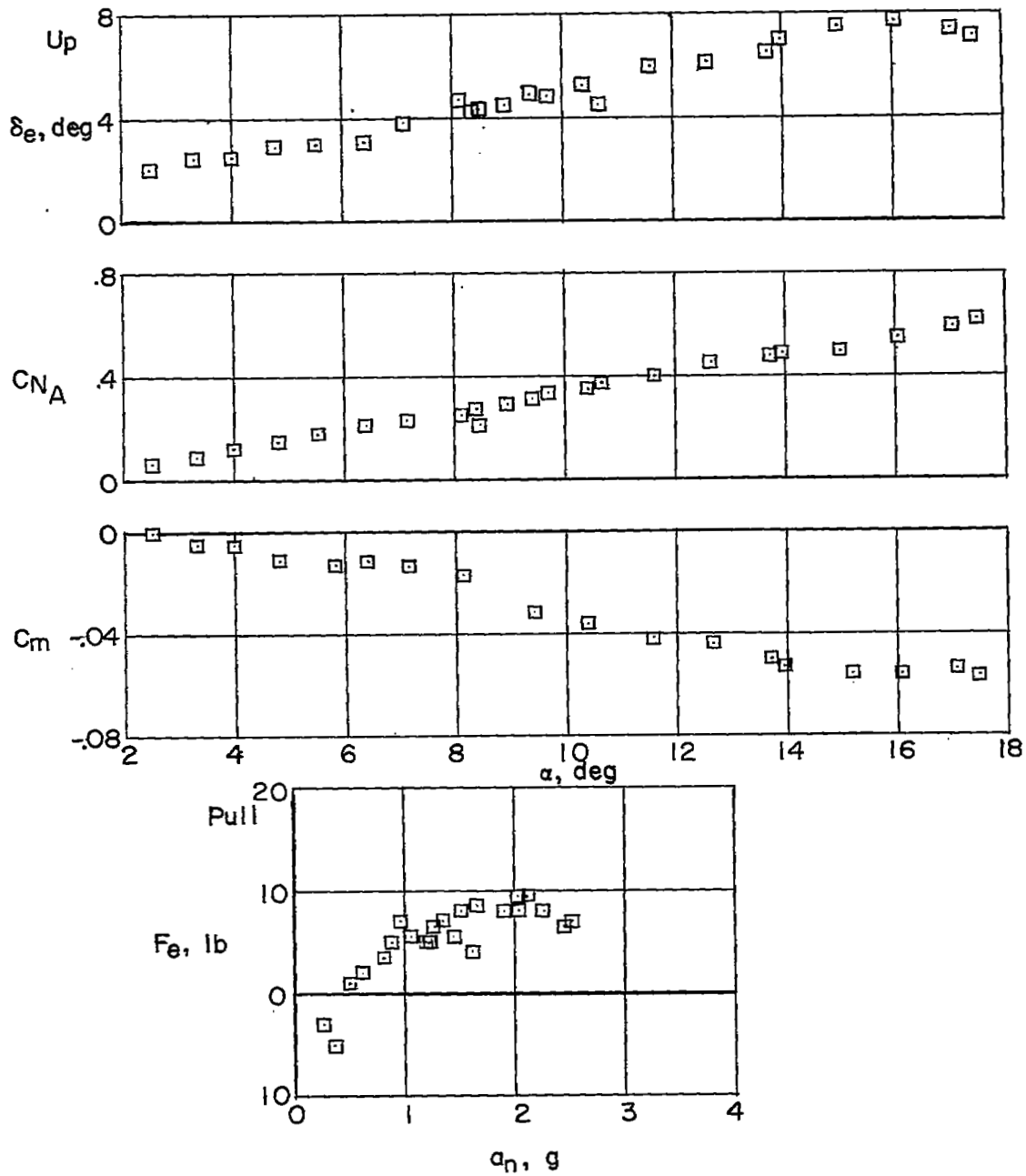
(c) $M \approx 1.13$; $h_p \approx 40,000$ feet.

Figure 9.- Continued.



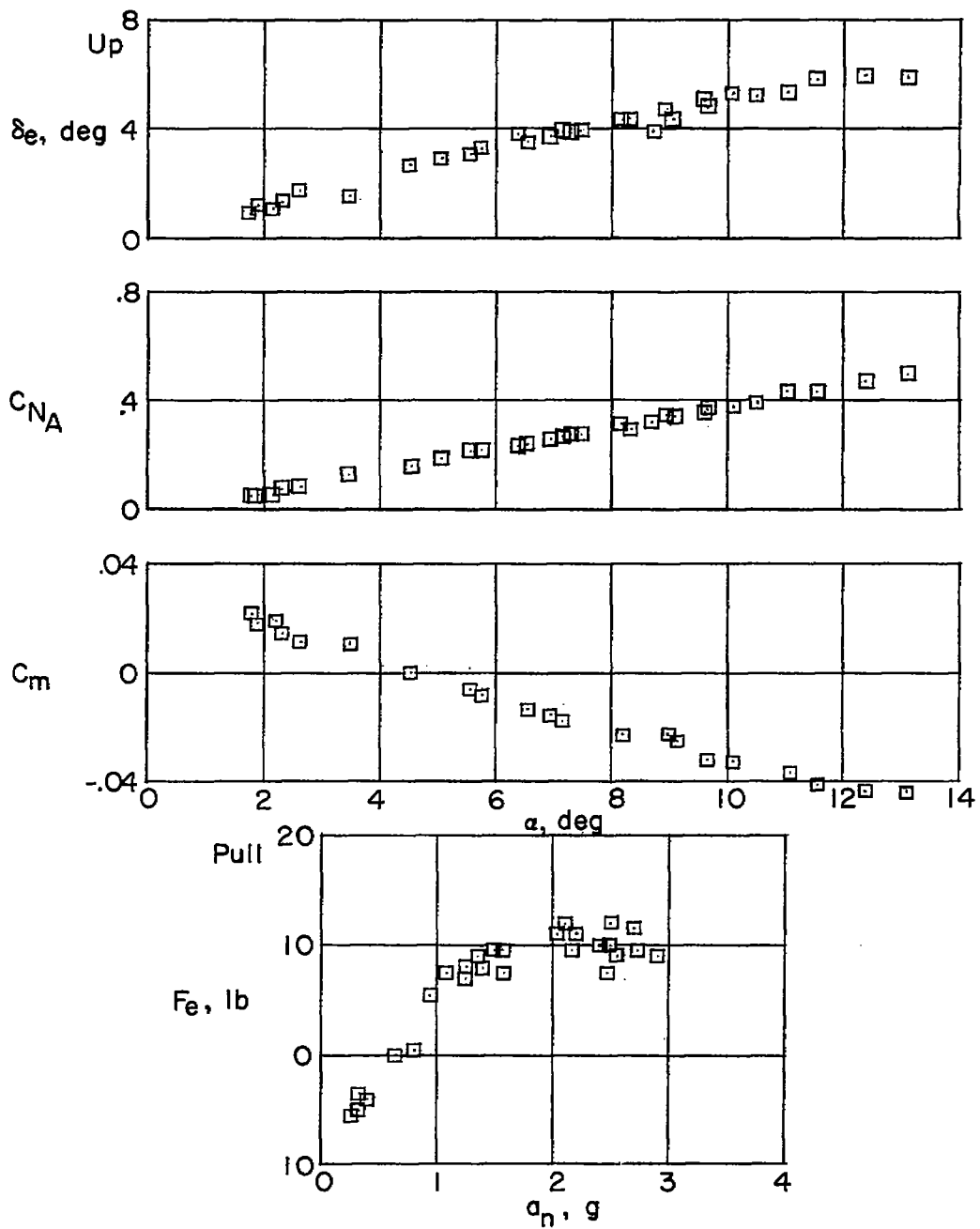
(d) $M \approx 0.93$; $h_p \approx 50,000$ feet.

Figure 9.- Concluded.



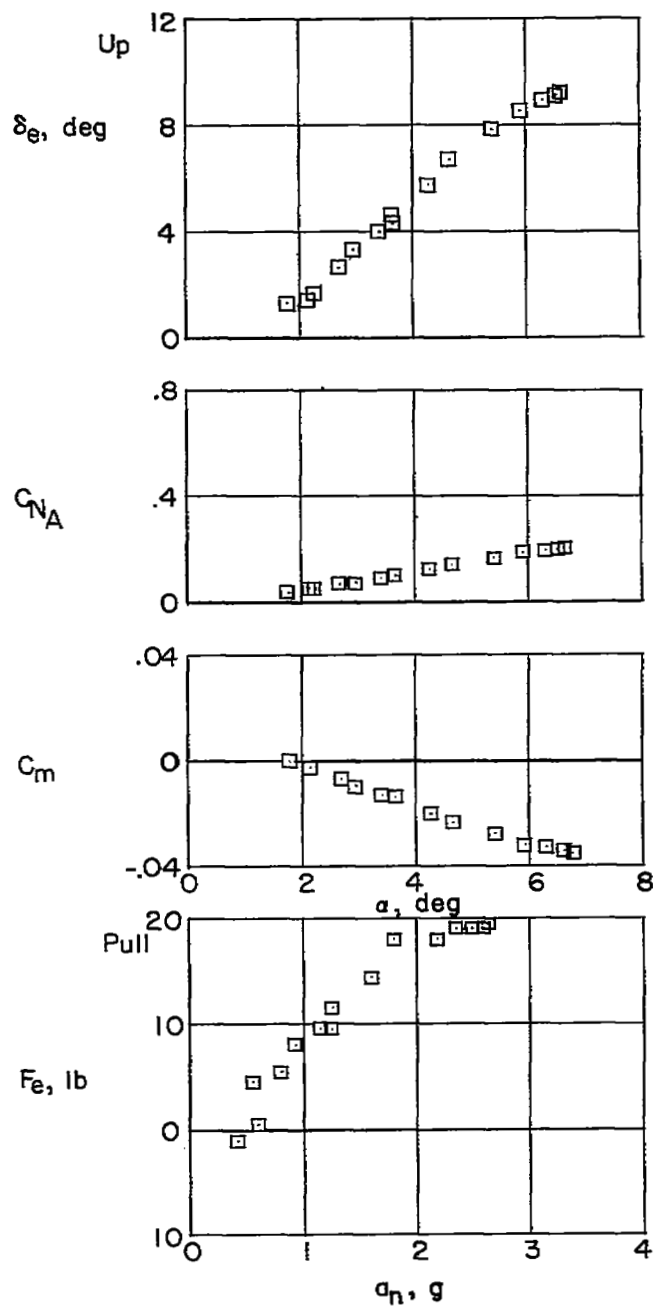
(a) $M \approx 0.70$; $h_p \approx 40,000$ feet.

Figure 10.- Representative stability plots of wind-up turns performed with the cambered-wing Convair YF-102 airplane.



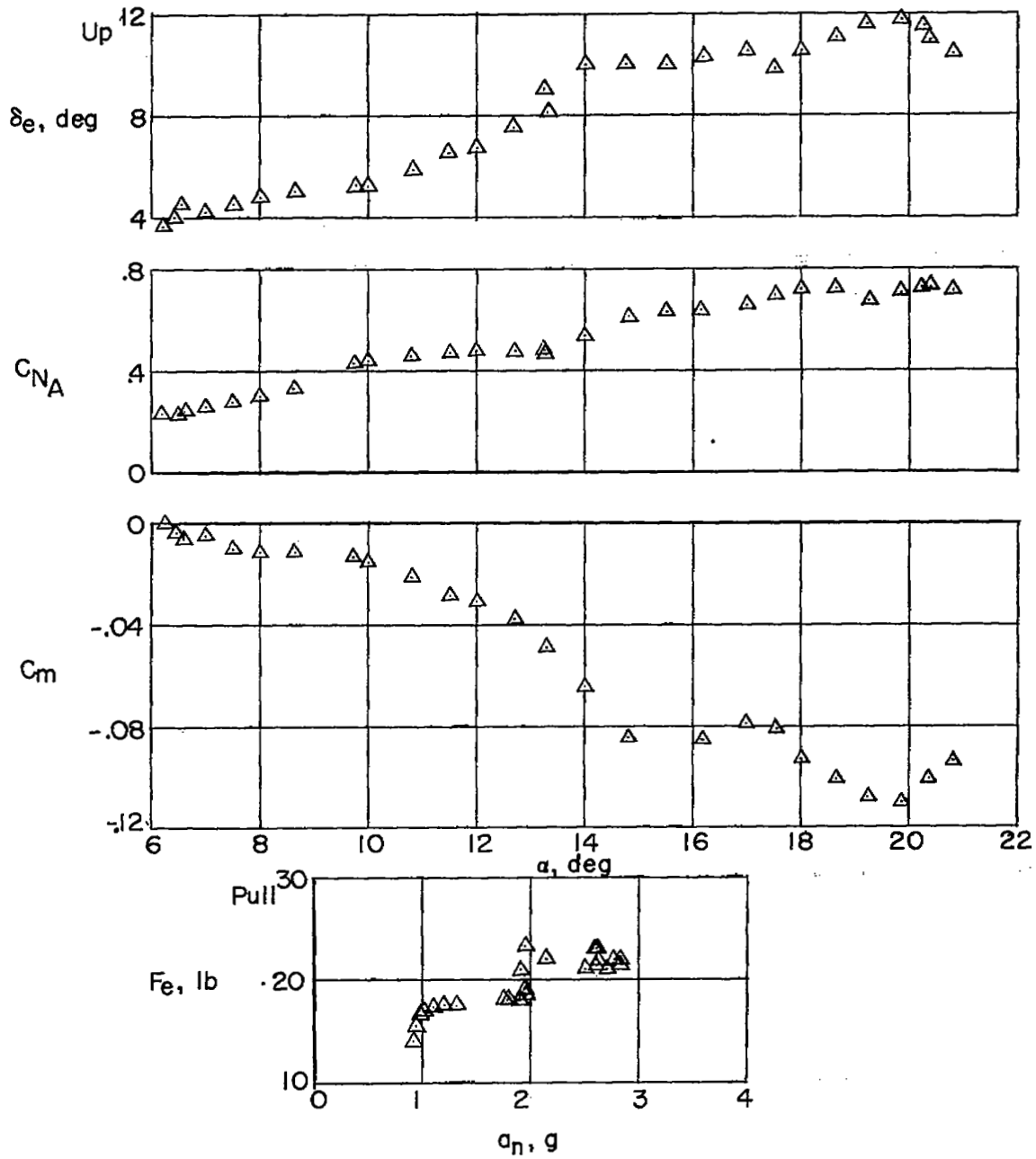
(b) $M \approx 0.89$; $h_p = 40,000$ feet.

Figure 10.- Continued.



(c) $M \approx 1.13$; $h_p = 40,000$ feet.

Figure 10.- Continued.



(d) $M \approx 0.93$; $h_p \approx 50,000$ feet.

Figure 10.- Concluded.

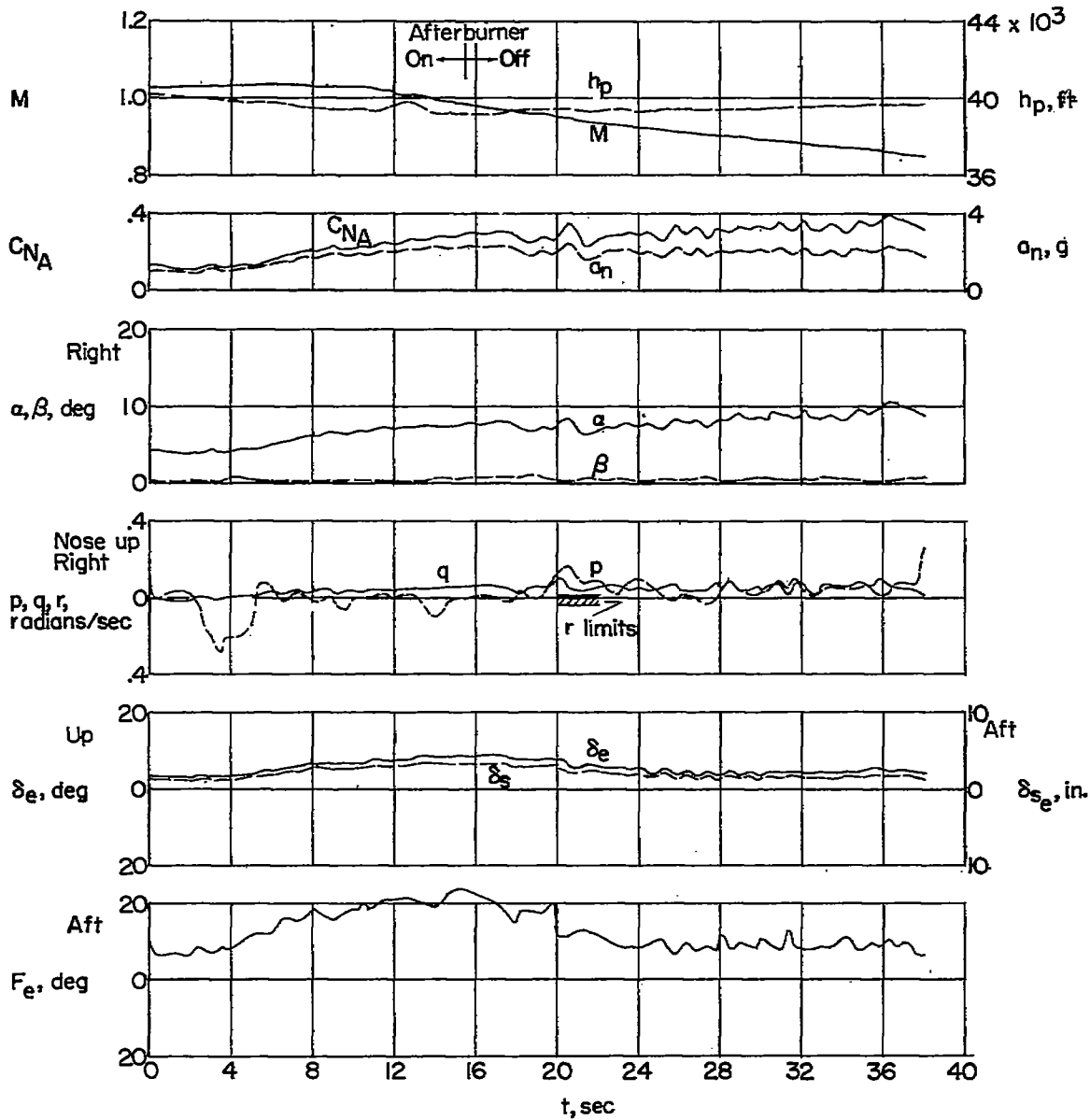
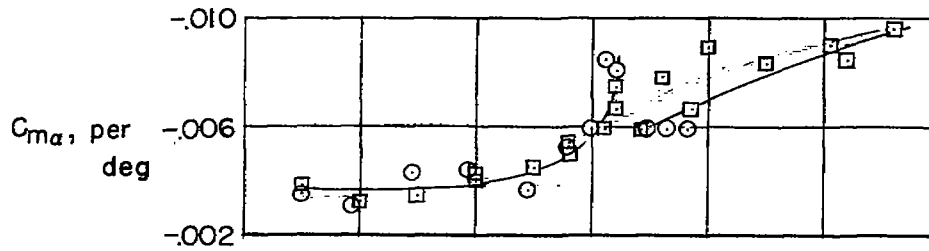
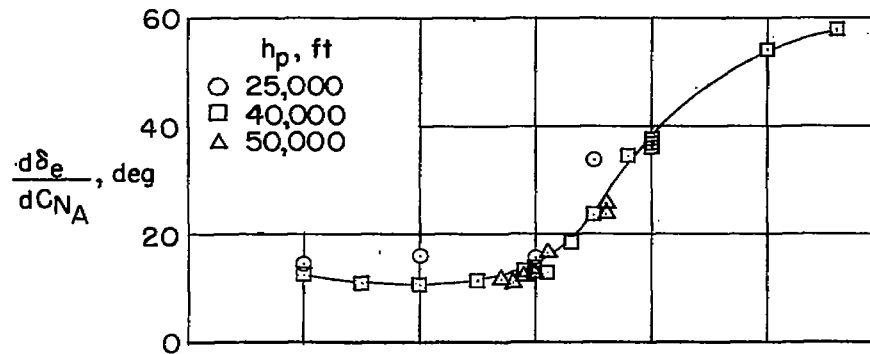


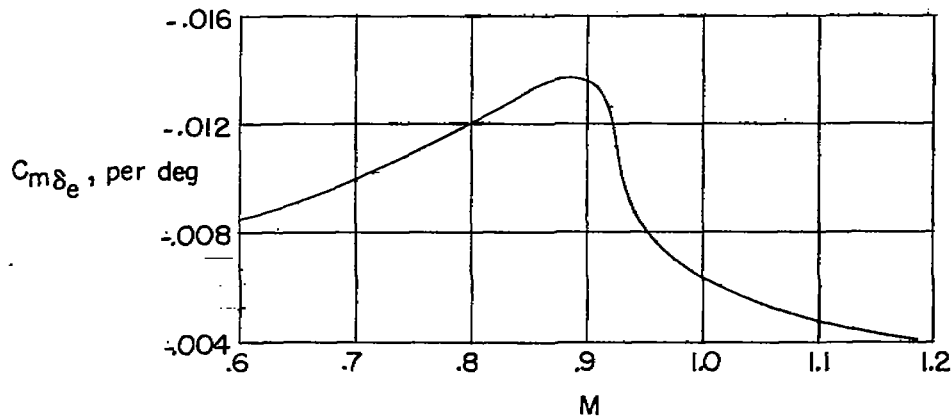
Figure 11.- Typical time history of a constant 2g turn performed by the YF-102 airplane to investigate the stability in the trim-change region with a rapid decrease in speed.



(a) Static stability.



(b) Apparent stability.



(c) Control effectiveness.

Figure 12.- Variation of the stability and control effectiveness parameters with Mach number for the cambered-wing Convair YF-102 airplane.

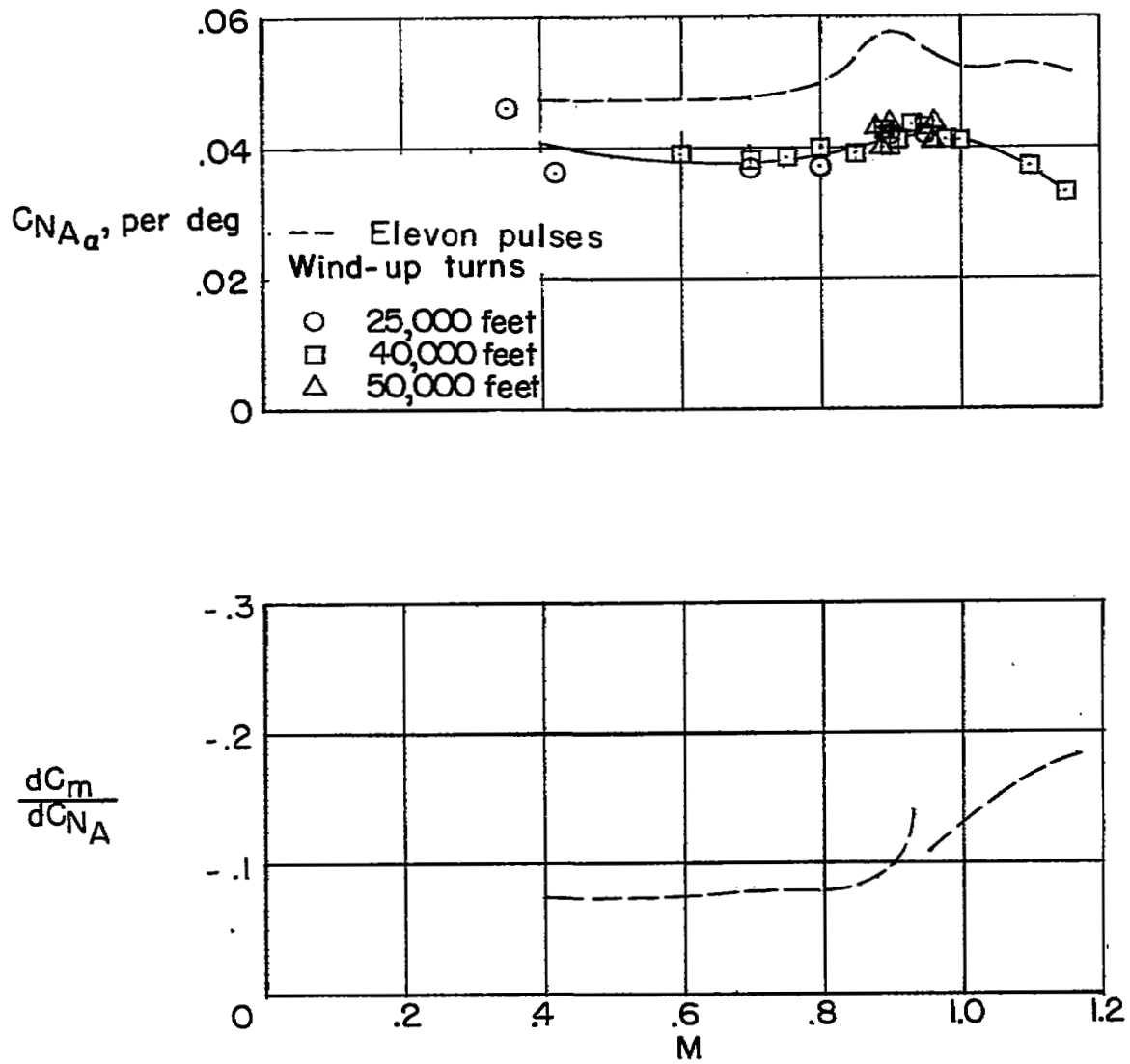
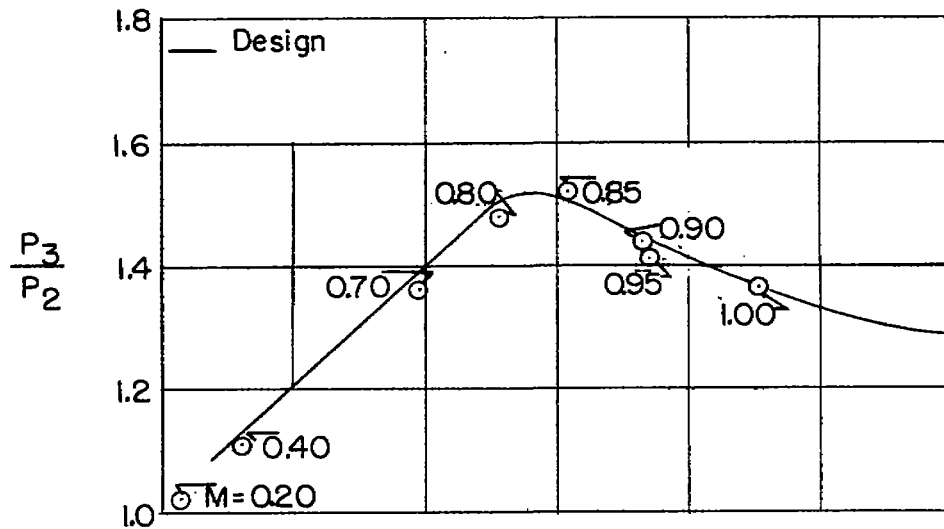
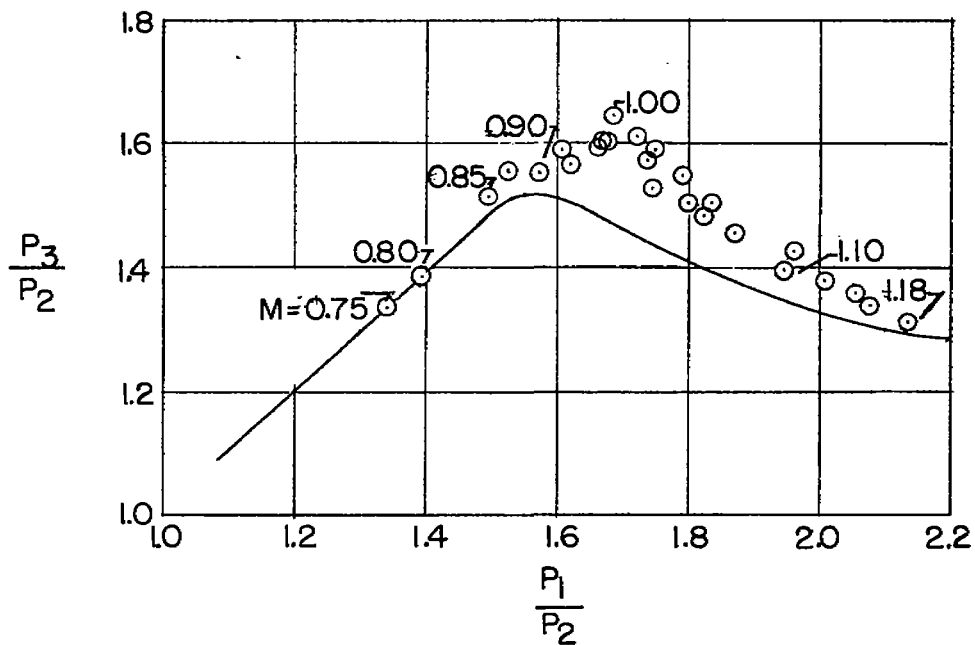


Figure 13.- Normal-force coefficient slope and static margin variation with Mach number for the cambered-wing Convair YF-102 airplane.



(a) Ground calibration.



(b) Flight data.

Figure 14.- Comparison of the design requirements and flight results for the artificial-feel system.

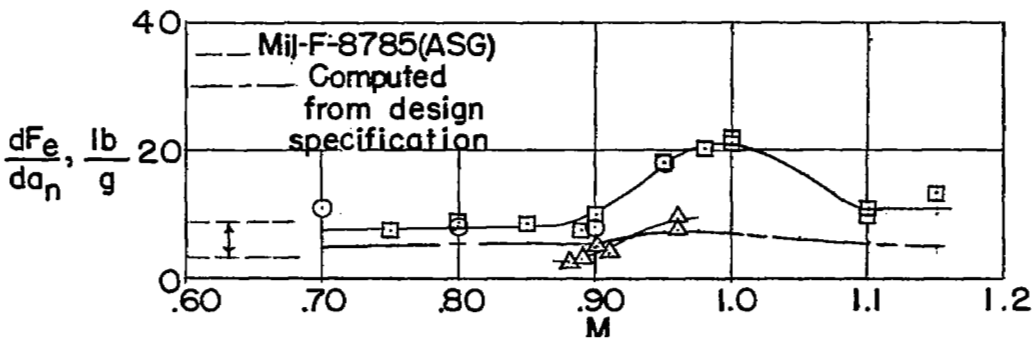
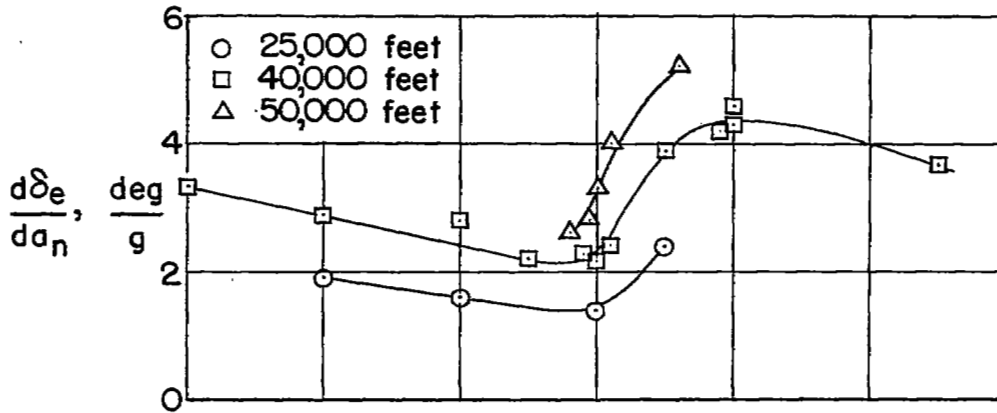
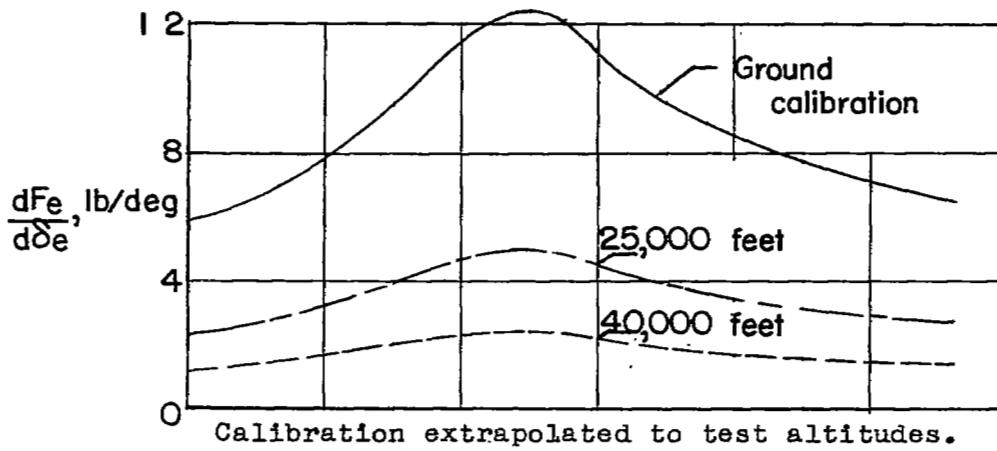
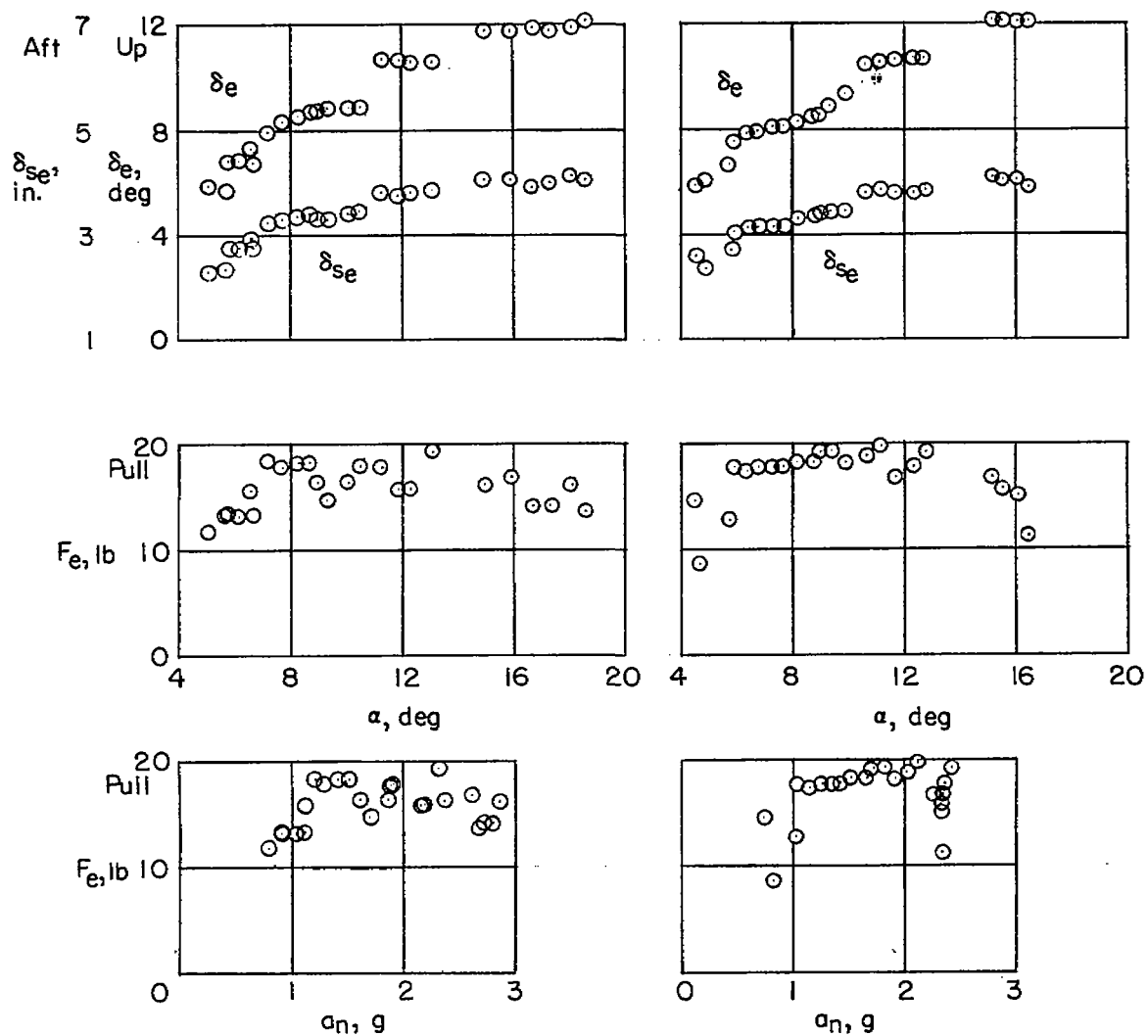


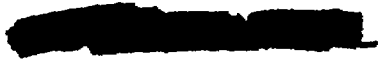
Figure 15.- Comparison of the design and flight-obtained force characteristics with the Military Specification of reference 2.



(a) Old static source.
 $M = 0.95$; $h_p \approx 50,000$ feet.

(b) New static source.
 $M = 0.95$; $h_p \approx 50,000$ feet.

Figure 16.- Characteristic effect of providing a more accurate static reference to the artificial-feel system.



NASA Technical Library



3 1176 01435 9997

